

# **For Reference**

---

**NOT TO BE TAKEN FROM THIS ROOM**

Ex LIBRIS  
UNIVERSITATIS  
ALBERTAENSIS











THE UNIVERSITY OF ALBERTA

RELEASE FORM

NAME OF AUTHOR ..Thomas Michael Morrow.....  
TITLE OF THESIS ..Sequential Hail Samples.....  
                            ..from Alberta Hailstorms.....  
                            .....  
DEGREE FOR WHICH THESIS WAS PRESENTED ..Master of Science.....  
YEAR THIS DEGREE WAS GRANTED .....1976.....

Permission is hereby granted to THE UNIVERSITY OF  
ALBERTA LIBRARY to reproduce single copies of this  
thesis and to lend or sell such copies for private,  
scholarly or scientific research purposes only.

The author reserves other publication rights, and  
neither the thesis nor extensive extracts from it may  
be printed or otherwise reproduced without the author's  
written permission.



THE UNIVERSITY OF ALBERTA  
SEQUENTIAL HAIL SAMPLES  
FROM ALBERTA HAILSTORMS

by

THOMAS MICHAEL MORROW



A THESIS

SUBMITTED TO THE FACULTY OF GRADUATE STUDIES AND RESEARCH  
IN PARTIAL FULFILMENT OF THE REQUIREMENTS FOR THE DEGREE  
OF MASTER OF SCIENCE IN METEOROLOGY

DEPARTMENT.....Geography.....

EDMONTON, ALBERTA

SPRING, 1976



Digitized by the Internet Archive  
in 2024 with funding from  
University of Alberta Library

<https://archive.org/details/Morrow1976>

THE UNIVERSITY OF ALBERTA  
FACULTY OF GRADUATE STUDIES AND RESEARCH

The undersigned certify that they have read, and  
recommended to the Faculty of Graduate Studies and Research,  
for acceptance, a thesis entitled.....  
.....SEQUENTIAL HAIL SAMPLES.....  
.....FROM ALBERTA HAILSTORMS.....  
submitted by ..Thomas Michael Morrow.....  
in partial fulfilment of the requirements for the degree of  
Master of Science  
in Meteorology.

---



## ABSTRACT

A method of collecting sequential samples of falling hail was developed and used during the summers of 1973 and 1974. The collectors were mesh screens and had collecting apertures of  $0.75 \text{ m}^2$  and  $0.58 \text{ m}^2$  respectively. The collected hailstones were stored in polyethylene bottles, plastic beakers or plastic bags. The collectors were operated from vans working in conjunction with the Alberta Hail Project. Samples were obtained from three storms in 1973 and six storms in 1974.

Several methods of analyzing the collected hailstones for hailstone numbers and size distributions were evaluated. The most commonly used technique was to count and measure manually photographs of the collected hailstone samples. Size distributions produced by this method gave results similar to those obtained from hailpads, and different to a greater extent from those obtained from photographs of the hail lying on the ground.

The resulting size distributions could be described by several density functions or distribution functions. An exponential density function

$$N(D) \delta D = 28,239 e^{-2.0D} \delta D$$

provided the best description of the size distribution of the hail collected during the two years. The function varied from year to year. It was



$$N(D) \delta D = 38,967 e^{-3.8D} \delta D$$

in 1973 and

$$N(D) \delta D = 6,427 e^{-1.8D} \delta D$$

in 1974. Exponential density functions of flux density and hailstone concentration were also calculated and compared with values found in the literature. A log-normal distribution was obtained for the collected hail. The log-normal distribution compared well with other log-normal distributions found in the literature when the hailstones considered were restricted to those with diameters greater than or equal to 0.5 cm. A power-law size distribution of the form

$$C(D) = k D^{-\alpha}$$

was tried. The values for  $\alpha$  varied from 0.13 to 7.1, with a value of approximately 3 for the 1974 hailstones greater than or equal to 0.5 cm only.

Three sets of hailstone samples from three differing hailstorms were selected for a time-dependent analysis. Time changes of size spectra, hailstone flux, hailstone concentration, hailstone mean and median size, and variance from an exponential distribution were studied. The largest hailstones fell during the time of greatest hailstone flux. The size spectra of the samples were



most nearly exponential during the times of greatest hailstone flux.

A simple hailshaft model was developed to predict upper-air hailstone concentrations by extrapolating backward in time the hailstone concentrations at the ground calculated from the collected samples. The model was applied to samples collected from a large hailstorm of 18 August 1974. The model indicated that the hail may have accumulated in the lower part of the updraft, and that the collected hailstones possibly came from two separate hail cells.



## ACKNOWLEDGMENT

Many people shared in the creation of this thesis. To them I wish to extend my appreciation.

Dr. E. P. Lozowski, my supervisor, willingly provided moral and financial support throughout these long years. In addition, his clear reasoning and red pens restrained and guided my somewhat erratic flights of fancy in a rational direction.

Drs. R. B. Charlton, K. D. Hage and E. R. Reinelt, other members of the Division of Meteorology, offered helpful advice and intelligent questions, which did not always receive intelligent answers.

Dr. G. G. Goyer of the Alberta Hail Project served as a member of my examining committee.

My fellow students, Alastair Beattie, Lawrence Cheng, Myron Oleskiw, Geoff Strong and Peter Wrenshall, assisted in the collection of the hail samples under the adverse conditions of Alberta hailstorms.

Dr. W. Davis and Norman Tsang of the Department of Computing Science provided their particle counting computer system for the analysis of the 1973 samples.

The Departments of Mechanical and Civil Engineering of the University of Alberta provided cold-room facilities.

The staff of the Alberta Hail Project provided accomodation and equipment in the field as well as expert radio direction in the pursuit of hailstorms.

This experiment was carried out with the financial support of the Atmospheric Environment Service of Canada.



\*\*\*\*\*

BIBLIOGRAPHY	87
APPENDIX I.        SAMPLING PROBLEMS	90
APPENDIX II.       MELTING OF FALLING HAILSTONES	93
APPENDIX III.      DETAILS OF INDIVIDUAL HAILSTONE SAMPLES	101
APPENDIX IV.       LOG-NORMAL DISTRIBUTIONS FOR INDIVIDUAL HAILSTORMS	111
APPENDIX V.        SIZE, FLUX DENSITY AND CONCENTRATION SPECTRA OF SEQUENTIAL HAIL SAMPLES	114



# LIST OF TABLES

TABLE		PAGE
1	Comparison of the two sequential sampling systems	12
2	Summary of the useful sequential storm samples	14
3	Comparison of the sample masses obtained by weighing and from measured images	19
4	Comparison of three hail size distribution sampling techniques used on 18 August 1974	21
5	Comparison of sample measurements obtained by measuring photographic images of hailstones and by measuring their longest dimensions with vernier calipers	22
6	Parameters of the best-fitting cumulative exponential distribution for hailstone samples collected from individual storms	33
7	Distribution parameters for individual sampling locations	43
8	Least squares fits for log-normal hail size distributions at individual sampling locations	45
9	Least squares fits for power law distributions of subsets of the concentrations of hailstone samples	50
10	Correlation coefficient R between number flux and mean diameter for three sets of storm samples	61
11	Correlation coefficient R between number flux and maximum diameter for three sets of storm samples	63
A1	Radius of a melting hailstone at the ground level after falling from the freezing level	98
A2	Liquid water content produced in the wake of a melting hailstone	99



## LIST OF FIGURES

FIGURE		PAGE
1	1973 Sampling System	7
2	1974 Sampling System	9
3	Cumulative size distributions of hailstone samples obtained in three different ways	21
4	Histograms of the cumulative size distributions of a hail sample taken from the ground near Forestburg, Alberta on 22 July 1974	22
5	Size distribution of a hail sample measured by the computerized line scanning system and by hand measurement of the photographic images	24
6	Hailstone size distributions for all sequential samples collected during 1973 and 1974	29
7	Oscillation of a cumulative exponential distribution caused by the superposition of several distributions with different characteristics	32
8	Hailstone size distributions for years 1973 and 1974 individually	34
9	Hailstone size distributions at single sampling points in individual storms 1973 and 1974	36
10	Size distributions of all sequential hail samples for the summers of 1973 and 1974 plotted on log-normal axes	41
11	Power law distributions of hailstones collected in 1974	48
12	Hailstone concentration vs. time and diameter, 9 July 1974	53
13	Hailstone concentration vs. time and diameter, 24 June 1974	54
14	Hailstone concentration vs. time and diameter, 18 August 1974	56
15	Number flux as a function of time	59



FIGURE		PAGE
16	Mass flux as a function of time	60
17	Mean and median diameters vs. time	62
18	Variance of sample distributions from an exponential distribution	64
19	$N_0$ of the best-fitting exponential distribution for concentration measurements	65
20	Temporal changes of $\Lambda$ and $N_0$ from Ulbrich (1974)	67
21	Wind shear and updraft profiles for the hailfall model	73
22	Isolines of hailstone concentration produced by the hailfall model above and upstream of a hail sampling site	76
A1	The effect of melting on a cumulative exponential distribution	100
A2	Hailstone size distributions at single sampling points in individual storms 1973 and 1974 on log-normal axes	112



During the summers of 1973 and 1974 the author was employed by Dr. E. P. Lozowski of the University of Alberta to assist in the operation of various field experiments performed in conjunction with the Alberta Hail Project (ALHAP). The work presented here resulted from the sequential hail sampling experiment performed during the two summers. This investigation covers three main areas:

1. the size distributions of the collected hail samples
2. the time-varying properties of the sequential samples
3. modelling the hailfall using the parameters of the collected hail samples.

Because the internal structure of the collected sample was not determined, whether or not the collected particles were actually hailstones also remained undetermined. For this study, the author applies the word "hail" to precipitation consisting of frozen water and disregards the differences between hail, frozen raindrops and graupel. This approach therefore sidesteps the question of whether hailstones smaller than 0.5 cm in diameter actually occur.

### 1.1 Size Distributions

Several attempts have been made to describe the size distribution of hail by a mathematical relation. The most prevalent



description is an exponential relation of the form

$$N(D) \delta D = N_0 e^{-\Lambda D} \delta D \quad (1)$$

where

$N(D) \delta D$  is the number of particles in a diameter interval  $D$  to  $D + \delta D$

$N_0$  is the y axis intercept of the resulting curve

$\Lambda$  is the negative slope

$D$  is the diameter.

Equation 1 also applies to rainfall (Marshall and Palmer, 1948).

Exponential distributions for Alberta hail are given by Douglas (1960, 1963, 1964). His samples were collected in wire mesh baskets and stored in freezers after the end of the hail-fall. This collection method may have resulted in the melting of some of the smaller hailstones in his samples. Equation 1 in Douglas' case was

$$N(D) \delta D = 40 e^{-2.93 D} \delta D \quad (2)$$

Ludlam and Macklin (1960) give an exponential distribution for hailstones from a severe hailstorm in England. The sizes were obtained from photographs of the hail lying on the ground after the passage of the storm. They give a value of  $\Lambda = 2.15 \text{ cm}^{-1}$  for their distribution.

Federer and Waldvogel (1975) obtained sequential hail samples from a Swiss hailstorm. The hailstone sizes were taken from a photograph of 30 seconds of hail collected on a foam rubber pad.



The mean distribution for the hailstones collected from this one storm was found to be

$$N(D) \delta D = 12 e^{-0.42 D} \delta D \quad (3)$$

Log-normal distributions are also applied to hail collections. Barge and Isaac (1973) give log-normal distributions for a sample of hailstones taken from 8 Alberta hailstorms in the summer of 1969. Since they were mainly interested in the shape features of the hailstones, their sample consisted mainly of large hailstones. In their paper, they also presented the data used in Douglas' exponential distributions in a log-normal form.

Another distribution encountered in the literature is a power law distribution of the form

$$C(D) = k D^{-\alpha} \quad (4)$$

where

$C(D)$  is the concentration of the hail in the diameter interval  $D - \delta D$  to  $D$

$D$  is the diameter.

Examples can be found in Auer (1972) for hail and graupel from convective cloud systems over the High Plains, and Auer and Marwitz (1972) for hail and graupel near a thunderstorm updraft.



## 1.2 Time-varying Properties

Although hailfall characteristics change greatly with time, some authors (List et. al., 1968; Charlton and List, 1972) model hailstorms as steady state phenomena. Douglas (1963) recognizes the problem in his discussion of size distributions: "The major source of error is likely to lie in the assumption that the size distribution remains invariant throughout the period of hailfall. Such invariance is most unlikely..."

Williams and Douglas (1963) report the observed differences in three parameters; rain/hail sequence, occurrence of largest hail, and continuity of hail. Because their results were derived from Alberta Hail Studies (ALHAS) hailcard reports, they were able to examine spatial variations as well as time variations.

Pell (1971) discusses the change with time and space of six hail parameters deduced from ALHAS hail card data. His results apply to the entire history of a hailstorm rather than being restricted to one point, so his conclusions do not relate directly to this study. He concludes that "...Alberta hailstorms seem to be most intense in their youth, becoming more and more dissipated as they pass middle age".

Ulbrich (1974) derived the two parameters,  $\Lambda$  and  $N_0$ , of an assumed exponential distribution along with the maximum diameter from Doppler radar spectra of falling hail. He states that the total hailstone concentration for all sizes decreased from  $1000 \text{ m}^{-3}$  to  $10 \text{ m}^{-3}$  and the median diameter increased from about 0.1 cm to about 1.0 cm during a period of observation of 8.5



minutes. With regard to  $\Lambda$  and  $N_0$ , he says "...the temporal behavior of  $N_0$  and  $\Lambda$  implies a size distribution which gradually broadens to hailstones of larger diameters and for which the number of smallest diameter stones is decreasing."

A sequential hail sampling experiment similar in concept to the one reported in this work was performed by Federer and Waldvogel (1975) in Switzerland. They were able to detect the passage of several hail cells during their collecting. Their results show that of an exponential distribution showed an increasing trend during the course of the storm.

Wisner et. al. (1972) present a time-dependent model of a hail-bearing cloud, in which they state, "...a steady state assumption is appropriate until the formation of hail in the cloud." The model assumes exponential raindrop and hailstone size distributions at all times and employs extensive parameterization of the microphysics. One of the properties was a vertical profile of hail concentration as a function of time. This output showed that the initial hail flux was small, rose to a maximum, then decreased to a minimum. The time of the maximum hail flux occurrence was influenced by melting and evaporation terms, but it was usually in the first half of the hailstorm lifetime. This theoretical result can be compared with the hail fluxes derived from this field experiment.



## CHAPTER 2      FIELD OPERATIONS

The sequential sampling experiment was planned to operate in conjunction with a mobile photography vehicle operated by the University of Alberta in cooperation with the Alberta Hail Project (ALHAP). The sampling experiment ran during the summers of 1973 and 1974. An account of the hail photography experiment has been given by Lozowski et. al. (1975).

The truck used during the summer of 1973 was a rented vehicle and modifications to it were not permitted. Consequently, the sampling equipment was of a very makeshift nature. The catcher consisted of a nylon mesh suspended about 70 cm above the ground by a light metal tubing frame (Figure 1). The nylon mesh had openings of about 0.5 cm. The relatively large mesh size was selected to allow rain to drain through quickly. No hail was ever observed to pass through the net. The net tapered to a spout in the center with an orifice diameter of 5 cm. Since any hail approaching that diameter would have destroyed the net, the spout was considered large enough to accomodate most of the hail expected to be encountered. The spout funnelled into the containers used for storage, which will be described later. The area of the collecting aperture was  $0.75 \text{ m}^2$ . The slope of the collecting surface was fairly flat, the surface being held in tension by the weight of the spout only. The resulting slackness of the netting prevented any significant bouncing of the





FIGURE 1. The 1973 sequential sampling equipment. In the foreground is the collapsible hail catcher. Below the catcher are several polyethylene bottles containing cooled hexane used to hold the collected hailstones. To the left of the picture is the styrofoam box which stores the sample bottles while in transit. The large white box seen in the back of the van is an extra freezer chest cooled by dry ice.



impacting hail. This catcher was collapsible and was carried along one wall of the van. When a stop was made for sampling or photography, it was set up in a convenient spot near the truck. Sampling could begin within 30 seconds of stopping the truck. No special effort was made to level the catcher, but it was probably within 5 degrees of horizontal in all sampling situations.

In 1974 the University was supplied with its own truck to which modifications could be made. The hail catcher was permanently mounted on the roof of the van, with the spout leading to the interior (Figure 2). A similar nylon mesh was used but with slightly larger openings (0.7 cm) and with a greater percentage of the netting filled in. This material was less desirable than that used the previous year with respect to the opening size and open area, but it was the best available at the time. Because of the permanent mounting of the new catcher, the net had to be stretched tightly to prevent sagging on the roof and accumulation of hail around the spout. Consequently, in order to prevent the hailstones from bouncing out, the net was given a steeper slope. The area of the catcher aperture was  $0.58 \text{ m}^2$  and it stood 1 m above the roof of the van and 2.7 m above the ground. The net led to a 7.5 cm opening in the roof and then to a flip-flop gate which could direct the hail to either one of two containers. This gate permitted the rapid changing of the sample containers at accurately controlled times.

Various means were used for storing the samples. The most





FIGURE 2. The 1974 sequential hail sampling equipment. The top photograph shows the hail catcher permanently mounted on the roof of the van. The lower photograph shows the interior equipment seen through the door on the right side of the van. At the top of the photograph is the catcher drain with two outputs. Below the clock is a microphone to the tape recorder. On the left side of the doorway is an electric freezer. The other equipment relates to the hail photography and air sampling equipment.



frequently used method was to collect the hail in 250 ml polyethylene bottles containing hexane cooled well below the freezing point of water by dry ice. This method of collection should very rapidly freeze any liquid water in the hailstone thereby preserving the crystal structure and overall mass of the hailstone. This "quenching" of the liquid water distinguished the spongy ice of the hailstone by transforming liquid portions into ice with many fine hairlike bubbles (Knight and Knight, 1968). A few problems were encountered with this method. Rain water is also collected along with the hail in spite of the holes in the mesh of the catcher, and the rain and hail tend to freeze into a single mass of ice at the bottom of the bottle. In a heavy shower, the bottle would fill up in about 10 seconds, leaving insufficient time for putting on the lid and storing the bottle before installing another. The hexane evaporates rapidly, and in spite of tight sealing of the bottles, they were frequently dried out when needed. This method was varied by using 400 ml plastic beakers with cardboard lids supplied by ALHAP. These were better than the bottles because of their increased capacity and quick lid operation, but the lids did not seal very well and spillage was common. For some storms (notably that of 18 August 1974) plastic bags were used. They had a large capacity, but the spongy ice was not quenched, and collected rainwater tended to melt the hailstones. An attempt was made to separate the rain from the hail in the beakers by inserting squares of metal screen in the beakers at the surface



of the hexane. The idea was that the hail would collect on the screen, while the rain would sink to the bottom of the beaker and displace the hexane up over the hail. Unfortunately, it did not work that way. The rainwater adhered to the surface of the hailstones, and the result was a frozen mass with a piece of screen imbedded in it.

In both years, the samples were stored in a styrofoam box cooled with dry ice and with a capacity of about  $0.1 \text{ m}^3$ . In 1974 the van was also equipped with an electric freezer that was used if the capacity of the box was exceeded.

Although both catchers were successful in collecting sequential samples, they had various disadvantages. The 1973 system was simple and relatively foolproof, but inconvenient and uncomfortable to operate. The 1974 system allowed better timing and faster operation, but the greater complexity increased the chance of mechanical breakdown. The 1973 net could be seen in operation, and interesting hailstones, as well as incipient trouble could be observed. The 1974 net was hidden from view and could become plugged up or torn without the operator immediately becoming aware of it. The 1973 system required a stationary operating location, while the 1974 system could be operated with the van in motion.

The timing of the sampling was done by wristwatch in 1973, while in 1974, a clock was installed near the output of the catcher. The timepieces were synchronized every few hours with the clock at ALHAP by means of radio time checks.



The containers were all numbered and the sampling times and numbers were recorded on a tape recorder. The tape recorder broke down a few times, with a resulting loss of the data. The tapes were subsequently transcribed for later reference.

Table 1 compares the two systems.

TABLE 1. Comparison of the two sequential sampling systems.

	1973	1974
Type	Portable, collapsible	Permanently mounted
Diameter of mesh holes (mm)	5.0	7.0
Area of collecting aperture (m <sup>2</sup> )	0.75	0.58
Height of collecting aperture above ground (m)	0.7	2.7
Maximum diameter of collectable hailstone (cm)	5.0	6.0
Time required to switch containers (s)	5	0.1
Minimum possible sampling time for one container (s)	15	1
Number of sampling days	6	13
Number of samples collected	58	79



The sampling vehicles used during the two summers operated together with the mobile sampling vehicles of ALHAP. These were directed into areas of high radar reflectivity as observed on the ALHAP radars. In 1974 the van was also equipped with a radio for monitoring the communications of the seeding aircraft and their controller. The procedure on a chase was to follow the instructions of the mobile controller at the radar console until the storm was in sight. Subsequently the course of action was determined by the observable features of the storm such as the precipitation shaft, cloud structure, and hail swath.

About 6000 miles were covered in obtaining hail samples during 1973 and 12,000 in 1974. The useful sequential samples are summarized in Table 2.



DATE	SAMPLING ONSET (MDT)	LOCATION	DURATION OF SAMPLING (minutes:seconds)	NUMBER OF SAMPLES
23 July 1973	19:41	NW S27T38R8W5	6:00	3
23 Aug 1973	19:50	SE S33T35R4W5	4:00	8
27 Aug 1973	15:23	NW S16T36R6W5	7:20	22
24 June 1974	15:54	NE S 9T31R3W5	5:00	6
2 July 1974	17:25	SE S26T38R3W5	1:00	4
5 July 1974	20:47	NW S36T38R2W5	10:00	6
9 July 1974	22:03	NW S 2T48R26W5	13:00	6
18 Aug 1974	17:21	SW S24T34R1W4	12:45	7
18 Aug 1974	17:49	S36T33R28W4	5:00	2
18 Aug 1974	18:10	SW S23T33R26W4	17:30	8
18 Aug 1974	18:42:30	S 1T33R25W4	3:00	2

TABLE 2. Summary of useful sequential storm samples. The location is specified by means of the Alberta Land Location System.



### CHAPTER 3. METHODS OF ANALYSIS

The analysis of the hailstones was carried out in the cold rooms of the Departments of Mechanical and Civil Engineering of the University of Alberta. The sequential samples that were used in the analysis are listed in Appendix 3. The primary objective of the analysis was to measure the numbers and external dimensions of the hailstones in each sample. Several methods were employed in performing these measurements.

The first attempt to determine the size distributions consisted of measuring each hailstone individually. However, holding the hailstones between the fingers melted them significantly and the very large numbers to be processed made this method quite impractical.

The next attempt consisted of photographing each sample spread out on a dark background, and counting and measuring the images. On the suggestion of Geoff Strong (private communication) the facilities of the Department of Computing Science were used for some of the counting. One of the students of the department, Norman Tsang (1974), applied a computerized scanning system to the counting of photographed articles. The procedure involved line scanning an enlarged photograph of the sample with a television camera, followed by digital processing of the video signal. The processed signal was used to reconstruct the photograph on



a monitor. The sensitivity of the system to different light levels from the photograph was adjustable, so that a good representation of the photograph could be obtained. The reconstructed display consisted of a grid of 2000 by 2000 points. Typically, the area photographed by the film camera was about 0.5 by 0.5 m, with the result that the resolution of the system was about 0.25 mm. The computer generated a number of rectangles, each one being just large enough to enclose a single particle image. The longest dimension of each of these rectangles was determined by the computer and a histogram of the size distribution of these longest sides was printed out. A source of error was introduced by the additional step of photographic enlargement from the negative. The blurring of the images, due to the film grain, added about a 20 percent uncertainty to the measurement of particles with a diameter of 1 mm.

Another major problem was the overlapping of hailstones in the photograph. Since the computer program could not always resolve an overlapped image into two separate hailstones, they were sometimes counted as a single larger hailstone. This problem was compounded by small ice chips and frost, which reduced the contrast of the photograph. In order to minimize this latter difficulty, most samples to be processed by the computer were sifted by a sieve with a 2 mm mesh size to remove the smaller particles.

This scanning system was used to count most of the samples collected during 1973. The exceptions were those with very few



hailstones which were easily counted and measured by hand, or those where the hailstones were frozen into a block with rain-water and could not be separated. These samples were analyzed by trying to distinguish the individual hailstones on a photograph of the frozen sample and subsequently counting and measuring the images by hand.

There were two major problems with the computerized system. One is the large error introduced by the inadequate resolution and contrast of the photographs. The other is the arbitrariness of the selection of the sensitivity level for the gray scale, which affected the detection of the small particles and the dimensions of the large hailstones. This system therefore was not employed for the 1974 samples.

The 1974 samples were photographed as before, but the negatives were projected onto a screen and the sizes of the hailstone images were measured by hand. The scale of magnification was adjusted so that the smallest particles of interest (about 2 mm diameter) could be measured with an accuracy of 20 percent. The hailstones were classified in size intervals of 1 mm. A ruler was included in all of the photographs to permit an accurate determination of the scale. The dimension measured was the longest linear dimension of the projected image. The reason for this procedure is as follows. A single ellipsoidal hailstone, under the influence of gravity, will most likely assume a position such that its longest dimension is parallel to the flat horizontal surface upon which it lies, and so parallel to the film plane.



The longest dimension is thus easily measured from the photograph. Further, it was frequently observed that if a hailstone was chipped, the chipping was such that the longest dimension of the hailstone tended to be the most preserved one, and therefore a better representation of the original hailstone than any other dimension. This anisotropic chipping of the hailstones appeared to result from the growth of large ice crystals with their long axes parallel to each other and parallel to the long axis of the hailstone. Since ice will tend to fracture along the boundary of a crystal, chipping on the short axes of hailstones would be possible. Finally, the longest dimension is a representative dimension for deposit and transfer calculations, according to List and Dussault (1967). The most serious drawback of using the longest dimension as a representative particle diameter is that it gives rise to misleading volume and mass estimates. This error is illustrated in Table 3. The samples were sequential samples from the storm of 18 August 1974 which contained from 10 to 100 hailstones each. The total mass of each sample was both measured directly and also calculated from the photographic distributions using the formula:

$$M = \sum_{k=1}^n N(D_k) \frac{\pi(D-0.5)^3}{6000} \rho_i \quad (6)$$

where

$n$  = number of millimeter size intervals considered

$N(D_k)$  = number of hailstones in size interval  $D_k$  to  $D_{k-1}$  mm



$D_k$  = image diameter in mm

$\rho_i$  =  $0.89 \text{ g cm}^{-3}$ , a typical density for hailstones.

TABLE 3. Comparison of sample masses obtained by weighing and from measured images.

SAMPLE	MEASURED MASS (g)	CALCULATED MASS (g)	RATIO
0880	53.3	59.8	1.12
0819	12.6	17.8	1.41
0883	4.5	6.1	1.36

The errors are caused chiefly by the non-sphericity of the hailstones which would lead to an overestimation of the sample mass calculated from the hailstone measurements. The presence of frozen rainwater in the collected samples on the other hand leads to an overestimation of the sample mass obtained by weighing. Both of these problems were extant on 18 August 1974, so the errors in Table 3 are probably the worst to be expected.

Another comparison of the relation of the longest image dimension to measurements from other sources can be obtained by comparing size distributions of hailstones from the storm of 18 August 1974 which were obtained in several different ways. Data for this comparison came from the hail catcher samples, from hailpads (Strong, 1974), and from photographs of the hail on the ground at the end of the storm. The measurements do not apply to the same hailstones, but to similar samples taken under similar conditions. The samples were separated in space by less than 5 meters, and were of the same 5 minutes of hailfall. Figure 3



shows the cumulative distributions of the samples measured by the three methods. Best-fitting straight lines were derived for the graph of the natural logarithms of the cumulative fraction of hailstones against their diameter. Table 4 shows three parameters of these straight lines for the various sampling methods. The hailpad measurements have been converted from dent size to hailstone size using the calibration curve of Strong (1974).

Table 4 shows that hailpads and the hail catcher give similar results. Using the longest dimension of a hailstone image as a representative dimension does not appear to result in errors in the size distribution exceeding those involved in the use of hailpads. Photographs of hail on the ground show more extreme differences from hailpads than the catcher samples do, possibly because the photographs were taken after the hail had ceased falling and when it had already melted significantly.

We will now compare size distributions obtained by measuring projected photographs of hail catcher samples with those obtained by measuring the longest dimension of the hailstones directly with calipers. The hailstones were collected from the ground near Forestburg, Alberta on 22 July 1974. Table 5 and Figure 4 compare the two methods of measuring the sample. The results show excellent agreement between the two measuring techniques. The sample consisted of relatively large hailstones. Smaller hailstones would be influenced by melting in the caliper measurements and the discrepancy between the two measuring techniques would be larger.



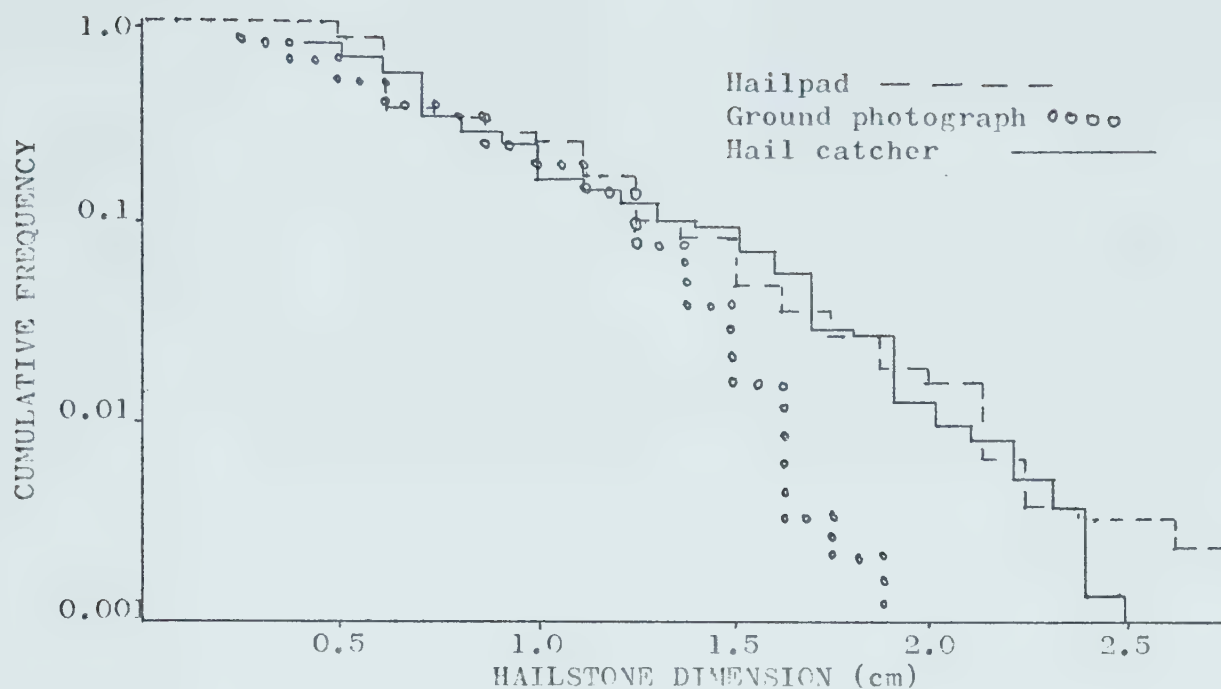


FIGURE 3. Cumulative size distributions of hailstone samples obtained in three different ways. DIMENSION is the hailstone diameter derived from the dent diameter for hailpads, the geometric mean of major and minor axes of the hailstone images for the ground photograph, and the longest dimension for the hail catcher.

Sample technique	$Y_0$	$M \text{ (cm}^{-1}\text{)}$	$s^2$
Hailpad	2.55	-2.75	$7.02 \times 10^{-3}$
Ground photograph	4.93	-3.36	0.102
Hail catcher	2.87	-2.69	$3.42 \times 10^{-3}$

TABLE 4. Comparison of three hail size distribution sampling techniques used on 18 August 1974.  $Y_0$  is the intercept of the best-fitting straight line with the Y axis.  $M$  is the slope of the straight line.  $s^2$  is the variance of the difference between the sample cumulative distribution and the straight line.



	<u>Number of hailstones</u>	<u>Mean diameter (cm)</u>	<u>Standard Deviation(cm)</u>
Hand measurement	40	1.81	0.35
Image measurement	40	1.78	0.39

TABLE 5. Comparison of sample measurements obtained by measuring photographic images of hailstones and by measuring their longest dimensions with vernier calipers.

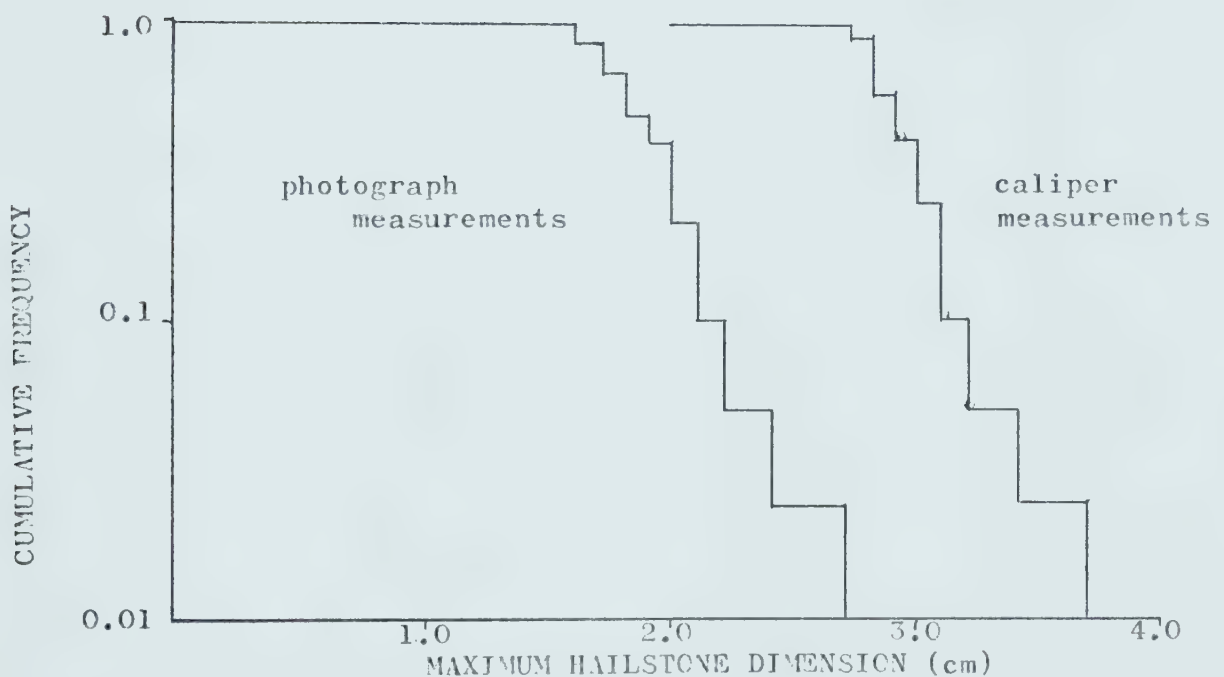


FIGURE 4. Histograms of the cumulative size distributions of a hail sample taken from the ground near Forestburg, Alberta, on 22 July 1974. The caliper-measured histogram is displaced to the right a distance of 1.0 cm along the x axis.



Knowing the accuracy of the measurements obtained using the projected images, the accuracy of the measurements obtained by the computerized line-scanning system can now be estimated. Figure 5 shows two histograms of hailstone size distributions for the same sample. One was obtained by measuring the photographic images manually, and the other was generated by the computerized line scanning system. The same photograph was used in both cases. The comparison is not very encouraging, because the total numbers and the modal sizes do not agree. The discrepancy is largely attributable to the overlapping of the hailstones, resulting in a large number of hailstones with a diameter of around 0.7 cm being counted as a smaller number of hailstones with diameters from 1.0 to 1.1 cm, by the computer. The larger numbers of particles in the 0 to 0.2 cm range counted by the scanning system are small ice fragments and frost particles that can be recognized and discounted when working manually. The number of hailstones counted by the scanning system was 111, while there were 179 counted by hand. These errors were discovered quite late in this work, and could not be corrected due to the poor focussing and lack of contrast in the photographs of the samples. Consequently, the size distributions for 1973 should be viewed with caution.

In some cases, the samples were too conglomerated with frozen rainwater to permit separation of all the hailstones. When this happened, as many hailstones as possible were separated and photographed. The mass of the separated hailstones was then



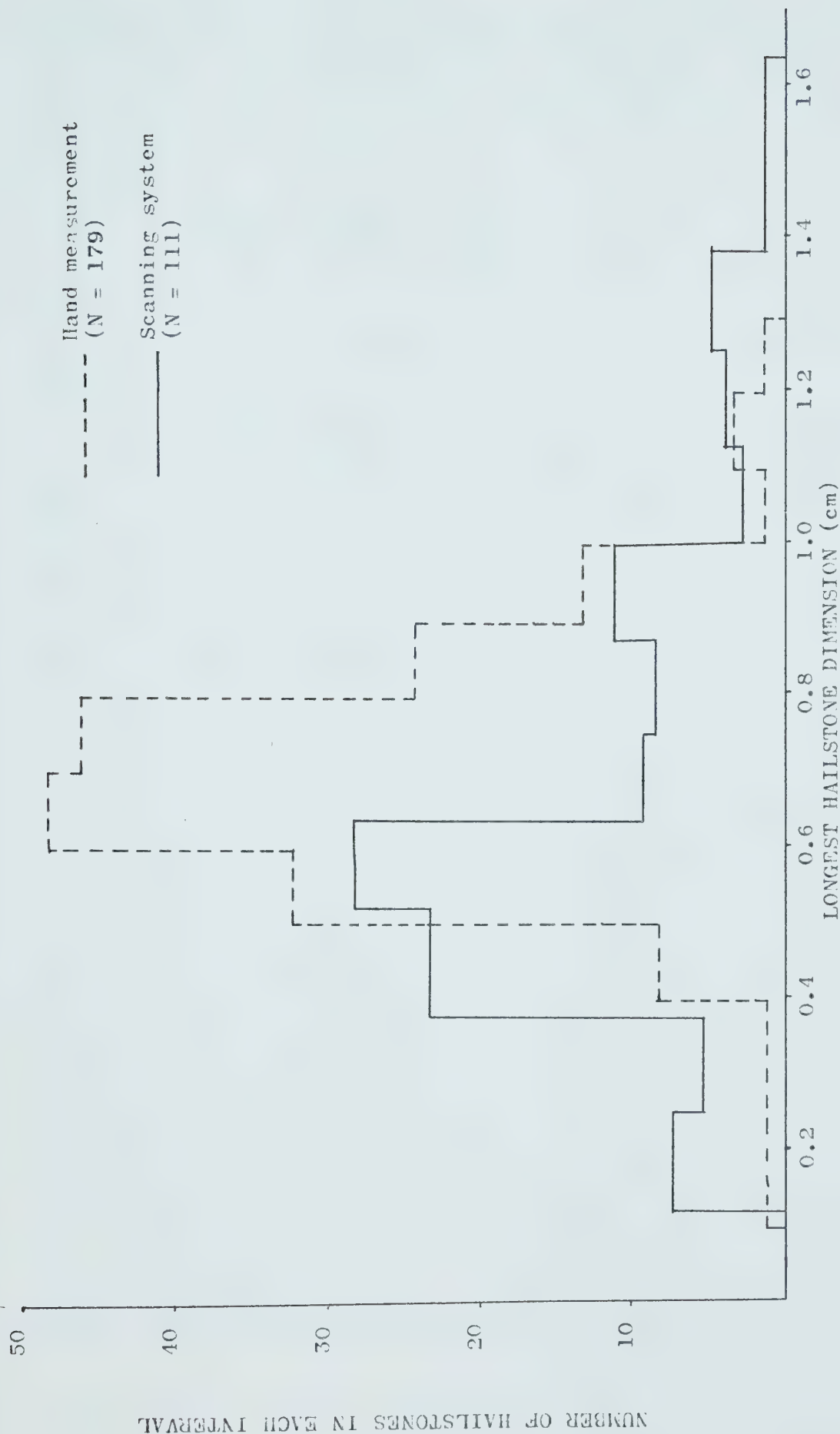


FIGURE 5. Size distribution of a hail sample measured by the computerized line scanning system and by hand measurement of the photographic images. N is the total number of hailstones counted by each method.



measured as well as the total sample mass. The final number of hailstones in each size category was then estimated using the formula:

$$N_d = N_{dp} \cdot \frac{M_s}{M_p} \quad (7)$$

where

$N_d$  is the estimated number of hailstones of diameter  $d-1$  to  $d$  in the entire sample.

$N_{dp}$  is the number of separated and photographed hailstones in the diameter interval  $d-1$  to  $d$

$M_s$  is the measured mass of the total sample

$M_p$  is the measured mass of the separated and photographed hailstones.

This was not an entirely satisfactory procedure, because the frozen conglomerate consisted largely of rainwater and the smaller hailstones, while the larger hailstones with less mutual contact area would be less likely to stick together and would therefore predominate in the separated hailstones. Thus, the estimated distribution is likely to have an excess of large hailstones, but no way was seen to correct for this. In some cases, the procedure adopted was to prepare a few cross sections of the lump, and to measure the sizes of the individual hailstone cross-sections. Although the slice may not have passed through the center of all the hailstones in the section, enough embryos were recognizable to indicate many hailstones that had been cut close to their center. Using these hailstones with recognizable embryos,



reasonable size distributions could be obtained. Of course this procedure does not give the number of hailstones in the entire sample, but an estimate can be made based on the sample mass, provided there is not too much rainwater in it. The samples from 9 July 1974 were those most affected by large amounts of rainwater.

There are two conclusions from this chapter that are important for the following work. First, the hail catcher and subsequent storage and analysis can produce results in hail size distributions comparable to those from hailpads. Secondly, the diameters of hailstones may be represented by their longest dimensions without unreasonable errors. For the remainder of this work, the term diameter will be used to mean the longest dimension of a hailstone.



## CHAPTER 4. SIZE DISTRIBUTIONS

### 4.1 Exponential Distributions

One way of representing size distributions of precipitation particles is by means of an exponential density function of the form:

$$N(D) \delta D = N_0 e^{-\Lambda D} \delta D \quad (8)$$

For example, Marshall and Palmer (1948) found for rainfall:

$$N(D) \delta D = 0.08 e^{-\Lambda D} \delta D$$
$$\Lambda = 41 R^{-0.21} \text{ cm}^{-1} \quad (9)$$

where  $R$  is the rainfall rate in  $\text{mm hr}^{-1}$ .

If the density function is integrated, a cumulative distribution function is the result:

$$N(D) = \int_D^{\infty} N(\mu) d\mu = \frac{N_0}{\Lambda} e^{-\Lambda D} \quad (10)$$

where

$N(D)$  is the number of particles with diameter  $\geq D$

$N_T = N_0/\Lambda$  is the total number of particles in the sample.

This is also an exponential distribution. The average diameter



of the sample is given by:

$$\bar{D} = \frac{\int_0^{\infty} DN(D) \delta D}{\int_0^{\infty} N(D) \delta D} = \frac{1}{\Lambda} \quad (11)$$

The mean volume is given by:

$$\bar{V} = \frac{\pi}{\Lambda^3} = \pi \bar{D}^3 \quad (12)$$

This is not the volume of a hailstone of mean diameter. The volume median diameter  $D_0$  is given by (Ulbrich et al., 1975):

$$2 \int_0^{D_0} D^3 N(D) \delta D = \int_0^{\infty} D^3 N(D) \delta D \quad (13)$$

The size distribution of all the hailstones collected in the sequential samples of the two summers is represented by the graph in Figure 6. This overall distribution is not representative either of an entire storm or of all the storms during a single summer. However, it is probably a fair estimate of the "representative" hail spectrum for Central Alberta. A straight line was fitted to the measured points of the distribution by the method of least squares giving the following parameters for the cumulative exponential distribution:



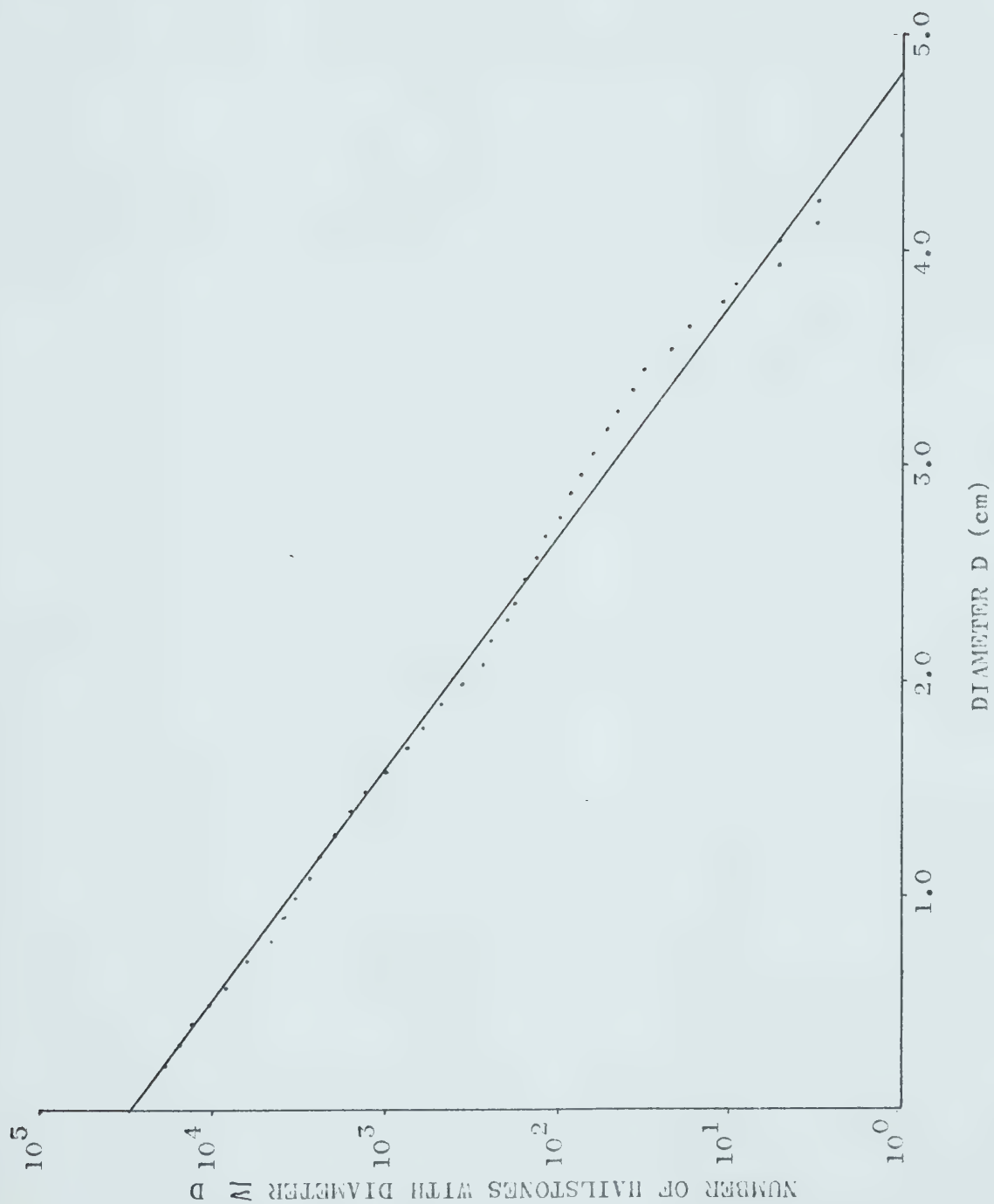


FIGURE 6. Hailstone size distribution for all sequential samples collected during 1973 and 1974. The points are the collected samples. The straight line is the best-fitting exponential distribution.



$$N_0 = 28,239$$

$$\Lambda = 2.0 \text{ cm}^{-1}.$$

The total number of hailstones in the sequential samples is then

$$N_T = N_0 / \Lambda = 14,056 \quad (14)$$

The variance of the collected sample distribution from the cumulative exponential straight line was calculated using the formula:

$$s^2 = \frac{\sum_{i=1}^n [(Y_i - \bar{Y}) - \hat{B}(D_i - \bar{D})]^2}{n-2} \quad (15)$$

where

$$Y_i = \log_{10} N(D)$$

$$\bar{Y} = \frac{1}{n} \sum_{i=1}^n Y_i$$

$$\hat{B} = \Lambda / \ln 10$$

and  $n$  is the number of size categories. The denominator  $(n-2)$  is used to obtain an unbiased estimate of  $s^2$  in the case where two parameters,  $\hat{B}$  and  $\hat{\alpha} = \bar{Y} - \hat{B}\bar{D}$  are estimated. The resulting variance was  $s^2 = 0.0199$ .



The main discrepancy between the least squares line and the sample points in Figure 6 occurs for diameters greater than about 2.5 cm. There are several possibilities for this discrepancy, assuming that an exponential distribution represents the "true" distribution of the hailstones from which the sample was drawn.

1. Assuming that an individual sample has a double exponential size distribution, the oscillations may have been caused by the summation of several samples with different values of  $\Lambda$ . This is illustrated in Figure 7. The narrow distributions may occur for individual hailfalls and will be discussed later.

2. Because of the smaller numbers of the larger hailstones, random fluctuations in the numbers collected would produce relatively larger errors than for the smaller hailstones. But fluctuations in the numbers collected do not appear to be random at diameters greater than 2.5 cm. Instead, there is almost a continuous wave.

3. Almost all of the larger hailstones came from two sampling locations of 18 August 1974. On both of those occasions, the catcher net was torn, and some of the hailstones, both large and small, could have been lost. The collecting area lost due to the tears was probably less than 40 percent.

An exponential distribution was fitted to the samples for each year and for each sampling location with the results shown in Table 6 and in Figure 8. The maximum size of hailstone collected in 1974 was about twice that of 1973, while the total number of hailstones collected during 1973 was almost three times



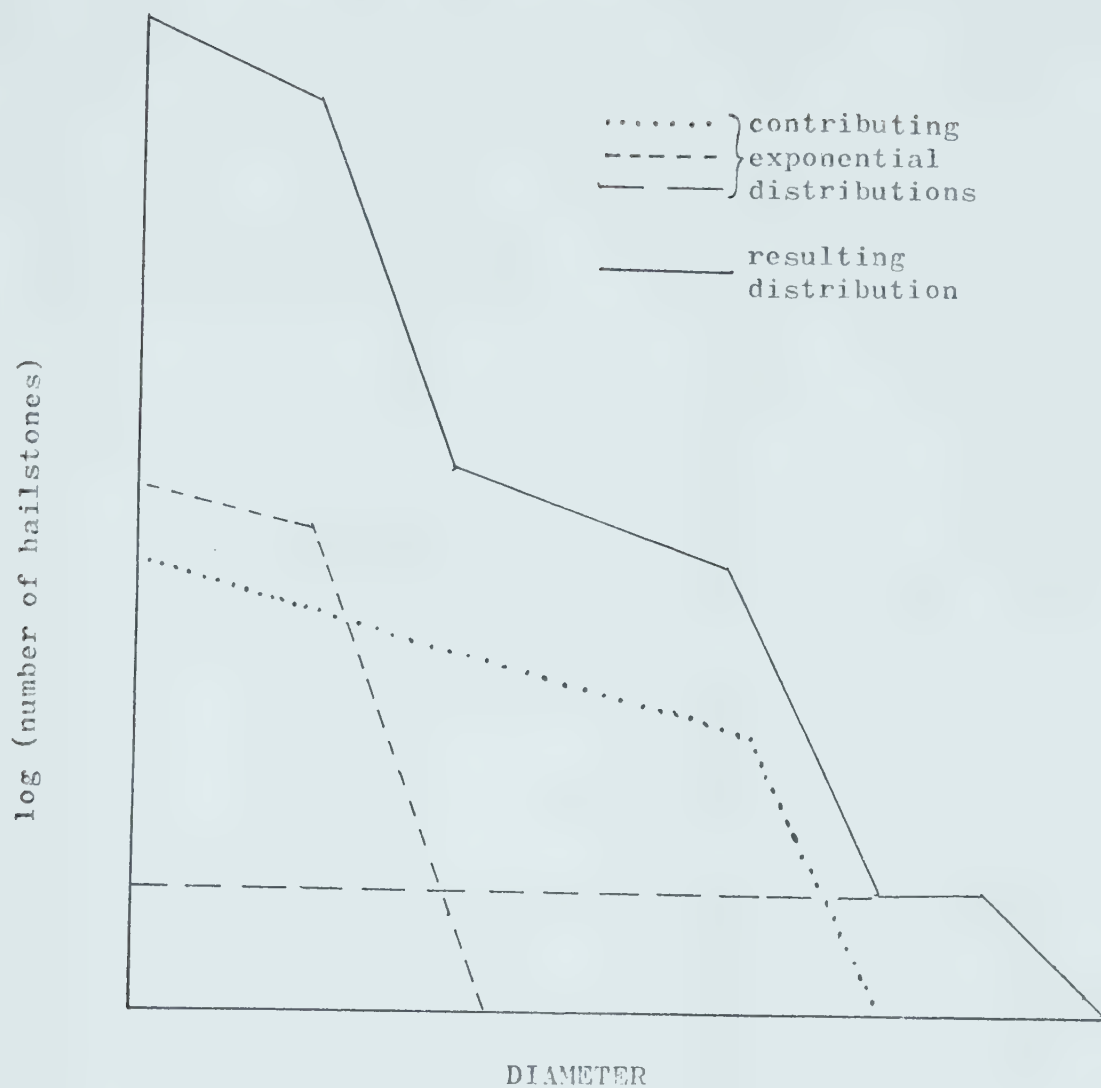


FIGURE 7. Oscillation of a cumulative exponential distribution caused by the superposition of several distributions of differing characteristics.



SAMPLE DATE	$N_T$	$(\text{cm}^{-1})$	$N_O (\text{cm}^{-1})$	VARIANCE
ALL	14,056	2.01	28,239	0.0199
1973	10,383	3.75	38,967	0.02
1974	3,673	1.75	6,427	0.03
23 July 1973	970	4.01	3,766	0.02
23 Aug 1973	3,314	3.52	11,705	0.02
27 Aug 1973	6,099	3.5	21,346	0.02
24 June 1974	147	2.83	416	0.09
2 July 1974	132	4.08	538	0.05
5 July 1974	717	5.83	4,177	0.04
9 July 1974	240	5.55	1,331	0.02
18 Aug 1974	312	1.08	337	0.08
18 Aug 1974	2,215	2.40	5,089	0.09

TABLE 6. Parameters of the best-fitting cumulative exponential distributions for hailstone samples collected from individual storms during 1973 and 1974.



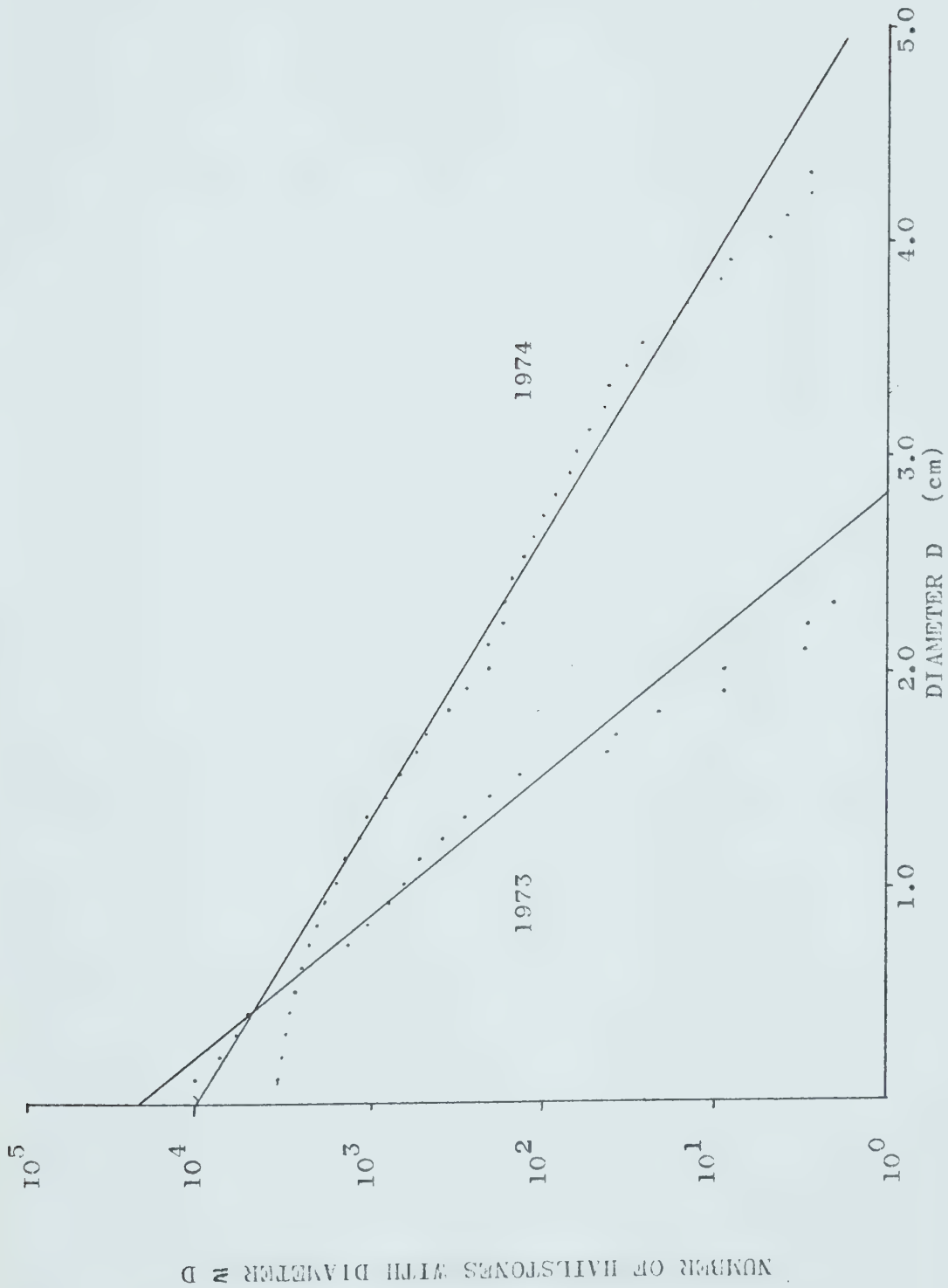


FIGURE 8. Hailstone size distributions for years 1973 and 1974 individually. The points indicate the collected samples. The lines are the best-fitting exponential distributions.



that collected in 1974. These differences can be attributed mostly to chance variations in the sampling occurrences and locations, rather than to climatological factors.

The results for the samples taken at single sampling sites in individual storms are also shown in Table 6. The values of  $\Lambda$  are generally greater in individual samples than they are for the total samples or for the yearly samples. This indicates that the size spectrum tends to be narrower for a single sampling location in an individual storm than it is for all the samples taken together. This fact is also pointed out by Auer and Marwitz (1972), who say: "...the size distribution of hail at a point from an individual storm is relatively narrow (almost monodisperse)....the Marshall-Palmer type of size distribution should not be expected throughout the storm." The cases observed in this work tend to corroborate the observations of Auer and Marwitz. The variance of the individual point samples from an exponential distribution is greater than that for the entire sample. This suggests, in agreement with Auer and Marwitz, that a cumulative exponential distribution is not as representative of a single-storm point-size distribution as it is of a sum of several hail samples. The relatively large variances of 0.08 and 0.09 for 18 August 1974 are perhaps indicative of the small number of hailstones collected, or of sorting by size by the torn catcher. The value of 0.09 for 24 June 1974 does not seem to be an experimental error, as that was one sampling occasion when everything worked well. Referring to Figure 9, it can be seen that the large variance results principally from a decrease



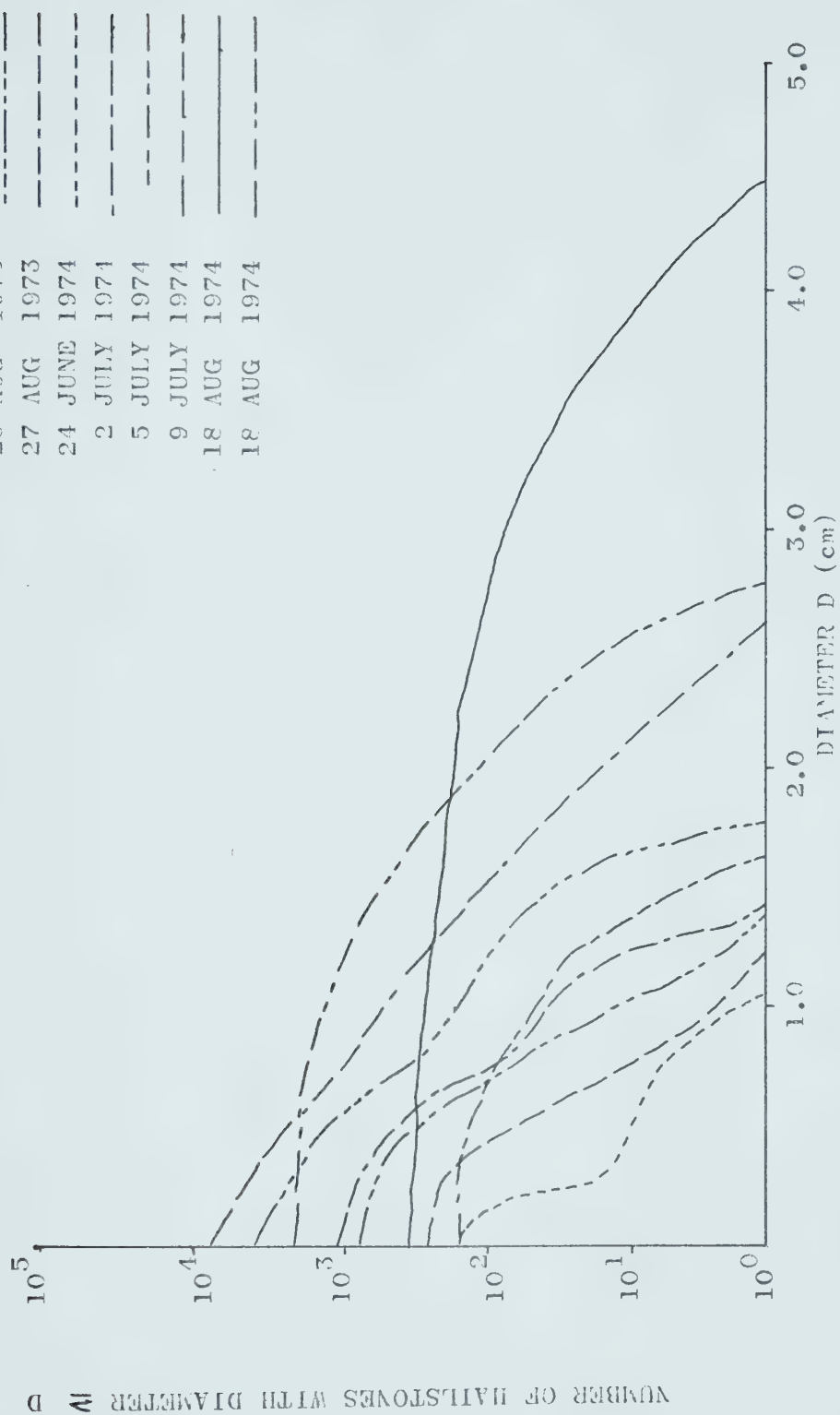


FIGURE 9. Hailstone size distributions at single sampling sites in individual storms 1973-1974. The parameters of the best-fitting exponential distributions are in TABLE 6.



in the number of hailstones from the expected exponential distribution number in the size categories from 0.3 to 0.6 cm.

One feature that may be seen from Figure 8 is the flattening of the 1974 distribution at the smallest sizes. This is also evident in the curves for the individual storm samples, shown in Figure 9. This feature is characteristic of many of the sample distributions and it is poorly described by the cumulative exponential distribution. Reasons for the absence of smaller hailstones were offered in Chapter 3. From personal observation, there seems to be a relative scarcity of the smaller hailstones at the ground. A possible explanation of the absence of small hailstones is melting below the freezing level of the storm. This hypothesis is considered in detail in Appendix 2. The conclusion is that melting can indeed remove some of the smaller hailstones from an initial exponential distribution at the freezing level. This also results in a change in the shape of the observed distribution.

Comparing the numbers of hailstones for each sample would be useful for estimating the relative intensities of different hailfalls during the sampling period. However, comparison of the total numbers is not very meaningful because the sampling times vary. This complication can be avoided by considering the mean flux density  $I$  of each sample:

$$I(D) = N(D) / A \delta t \quad (16)$$



where

$N(D)$  is the number of hailstones of diameter  $D$  to  $D + \delta D$  collected in a sampling time  $\delta t$ .

$A$  is the collector aperture area.

Values for  $A$  and  $\delta t$  are given in Chapter 2 and in Appendix 3.

The calculated values for the flux density of each sample are given in Appendix 3 and will be considered in detail in Chapter 5.

Exponential distributions were fitted to the flux density values using the least squares method. The parameters of these exponential distributions are given in Appendix 3. These results indicate a range of flux densities of over two orders of magnitude up to almost  $10^4 \text{ m}^{-2} \text{ min}^{-1}$ .

The mean concentration  $C$  of hail (number per cubic meter) is given by:

$$C(D) = I(D)/V_T(D) \quad (17)$$

where

$I(D)$  is the flux density calculated using Equation 16

$V_T(D)$  is the terminal velocity of hailstones of diameter  $D$ .

The terminal velocity of a hailstone can be estimated by equating the drag force and the weight of the hailstone:

$$V_T(D) = \left( \frac{4 \rho_i g}{3 C_D \rho_A} \right)^{\frac{1}{2}} D^{\frac{1}{2}} \quad (18)$$



where

$\rho_i$  is the density of the hailstone

$g$  is the acceleration of gravity

$C_D$  is the drag coefficient of the hailstone

$\rho_A$  is the density of air.

Values used in this work were  $\rho_i = 0.89 \text{ g cm}^{-3}$ ,  $g = 981 \text{ cm sec}^{-2}$ ,  $C_D = 0.5$ , and  $\rho_A = 1.05 \times 10^{-3} \text{ g cm}^{-3}$ . According to Strong (private communication) these are "representative" values for Central Alberta. This equation assumes spherical homogeneous hailstones. The concentration distributions at the ground for each sample are given in Appendix 3. The results for individual samples will be considered in Chapter 4.

An exponential distribution of hail concentration with size for a severe storm in England was found by Ludlam and Macklin (1959), who estimated size spectra from photographs of hail lying on the ground following the storm. Their equation for the concentration distribution in the air at ground level was:

$$N(D) = 40 e^{-2.15 D}$$

Because the hailstones may have melted on the ground before being photographed, tending to reduce the proportion of smaller hailstones, this equation may have a flatter slope than the true value. Douglas (1963) also gives an exponential size distribution for hailstones collected in several Alberta hailstorms. His sampling techniques, however, tended to emphasize the larger



hailstones in a sample. Consequently, the slope he derived ( $\Lambda = 2.93 \text{ cm}^{-1}$ ) may be smaller than the actual value which occurred in his sampling occasions.

#### 4.2 Log-normal Distributions

Another distribution used to describe collections of particles is the log-normal distribution, given by:

$$P(D) = \frac{1}{\sqrt{2\pi}} \int_{-\infty}^{u(D)} \exp\left(\frac{-u^2}{2}\right) du \quad (19)$$

where

$P(D)$  is the probability that a particle in the distribution has a diameter  $\leq D$

$$u = \frac{y - \bar{y}}{\sigma_y} \quad \text{is the standard normal variable}$$

$$y = \log_{10} D$$

$$\sigma_y = \left( \frac{\sum_{i=1}^n (Y_i - \bar{Y})^2}{n-1} \right)^{\frac{1}{2}} \quad \text{is the standard deviation of the } y\text{'s.}$$

Figure 10 shows the total sample population plotted on log-normal graph paper. The graph shows that 16 percent of the collected hailstones were smaller than 0.1 cm in diameter,



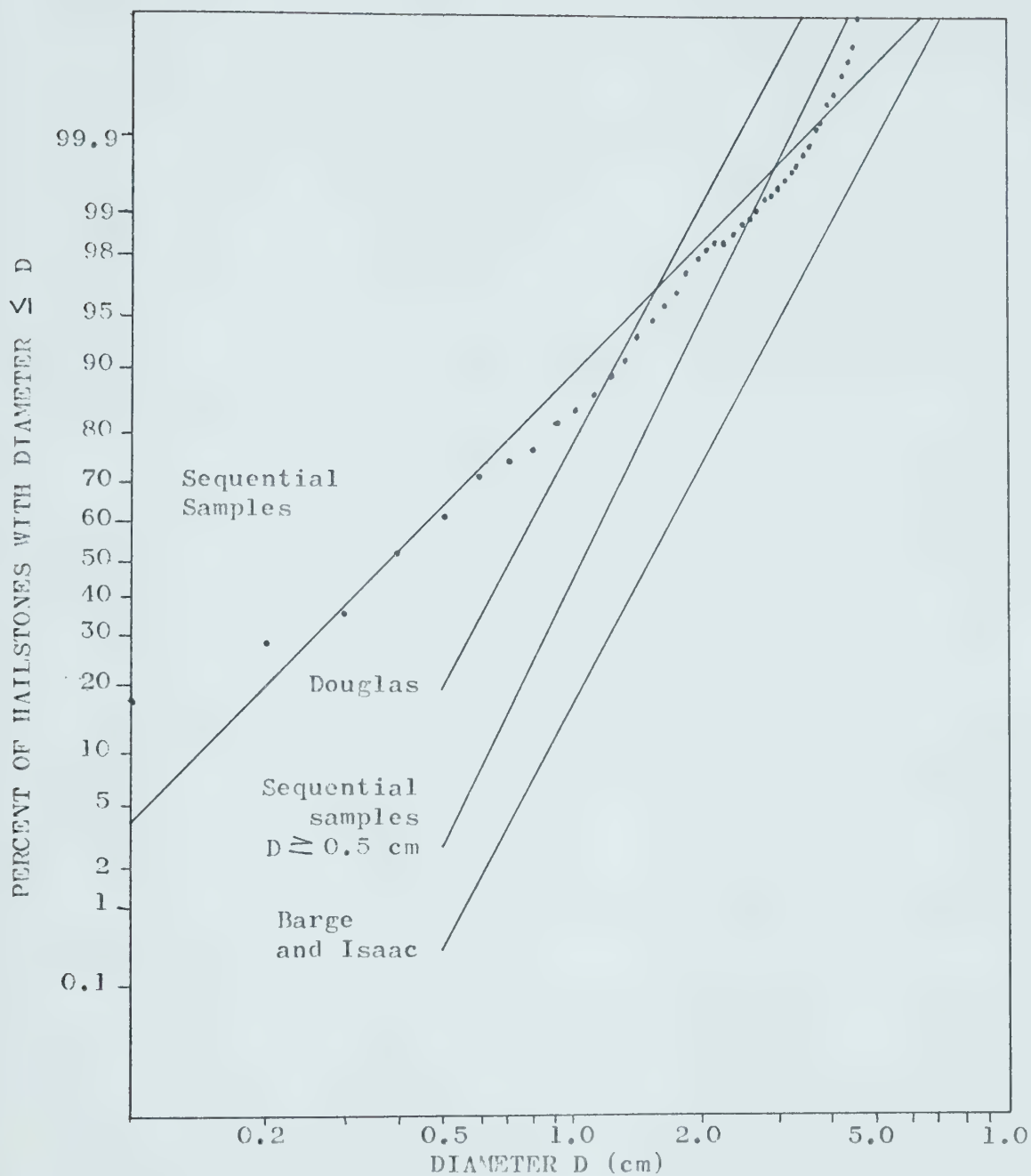


FIGURE 10. Log-normal size distributions of hail samples collected during 1973 and 1974, and by Douglas (1960) and by Barge and Isaac (1973). Also shown is the distribution of the hailstones from the sequential samples with diameters greater than 0.5 cm.



50 percent were smaller than 0.35 cm (the median size) and 90 percent were smaller than 1.2 cm. Corresponding to the oscillations of the curve in Figure 6 there is a "kink" in the graph for larger hailstones, in this case at a diameter of 2.0 cm. The graph seems to consist of two curved segments that approach some maximum diameter asymptotically. It should be emphasized that for  $P \geq 99.9$  percent on the graph, only ten or fewer hailstones are involved with the result that this part of the graph is not as reliable as the rest.

Also included in Figure 10 are log-normal distributions of other Alberta hailstorm samples. That due to Douglas consists of 67 hailstone samples (Barge and Isaac, 1973). The distribution due to Barge and Isaac (1973) was derived from 1920 hailstones collected from 8 Alberta hailstorms during the summer of 1969. If the hailstone samples of this work are reconsidered allowing only hail with a diameter greater than 0.5 cm (MANOBS), a distribution comparable to those of Douglas, and Barge and Isaac results.

Log-normal graphs of the sample size distributions of individual sampling occasions are shown in Appendix 4. Most of the graphs resemble Figure 10 in that they appear to consist of two curves connected at a kink. Some information about the hail sizes for each sampling location is given in Table 7. Particles smaller than 0.1 cm appeared in the samples on all but three occasions. The fraction of particles less than 0.1 cm in diameter usually varied between 0 and about one fourth of the total collected sample.



SAMPLE DATE	MINIMUM COLLECTED DIAMETER (cm)	FRACTION COLLECTED ≤0.1 cm	MEDIAN DIAMETER (cm)	MEDIAN VOLUME DIAMETER (cm)	90% DIAMETER (cm)
ALL	0.1	0.17	0.37	1.12	1.2
1973	0.1	0.22	0.31	1.07	0.74
1974	0.1	0.03	0.84	1.24	1.7
23 July 1973	0.1	0.14	0.33	1.07	0.57
23 Aug 1973	0.1	0.20	0.28	1.01	0.77
24 June 1974	0.3	0	0.75	1.24	1.10
2 July 1974	0.1	0.58	0.07	-	0.20
5 July 1974	0.1	0.04	0.34	1.06	0.63
9 July 1974	0.1	0.05	0.26	0.91	0.55
18 Aug 1974	0.4	0	1.9	1.28	3.3
18 Aug 1974	0.4	0	1.1	1.24	1.7

TABLE 7. Log-normal distribution parameters for individual sampling locations.  
The 90 % diameter is the diameter greater than or equal to 90 % of the collected sample.



The probabilities and diameters of the cumulative size distributions of the samples were transformed to two new variables, X and Y, using:

$$\begin{aligned}
 X &= \log_{10} D \\
 Y &= \frac{1}{\sqrt{2\pi}} \int_{-\infty}^u \exp\left(\frac{-u^2}{2}\right) du \\
 u &= \frac{X - \bar{X}}{\sigma_x}
 \end{aligned}
 \tag{20}$$

The transformed data were used to generate least squares fits to the graphs of Figure 10 and Appendix 4 in order to determine the parameters of the log-normal distribution most closely approximated by the data points. Table 8 gives the results of the calculations. The table shows that the slopes are not constant. According to List et. al. (1972), a constant slope means a constant standard deviation of the samples. This illustrates the lack of similarity among the samples from each location. As will be shown in Chapter 5, the standard deviation also varies during a hailfall. The two samples with the closest fit to a log-normal distribution (minimum variance from a log-normal distribution) are that of 9 July and the second sampling location of 18 August 1974. On these two occasions, rather large problems arose in the collection of the samples. On



SAMPLE DATE		SLOPE ( $\text{cm}^{-1}$ )	$P(D \leq 0.1 \text{ cm})$	VARIANCE
	ALL	3.034	0.04	0.055
	1973	2.994	0.0571	0.120
	1974	3.729	0.0009	0.146
23	July 1973	3.794	0.0465	0.115
23	Aug 1973	3.194	0.112	0.138
27	Aug 1973	3.443	0.0582	0.112
24	June 1974	7.339	0	0.262
2	July 1974	2.276	0.5948	0.193
5	July 1974	4.967	0.0080	0.109
9	July 1974	4.505	0.0307	0.048
18	Aug 1974	4.434	0	0.416
18	Aug 1974	7.093	0	0.087

TABLE 8 Least squares fits for log-normal hail size distributions at individual sampling locations.  $P(D \leq 0.1 \text{ cm})$  is the probability that a hailstone will have a diameter less than 0.1 cm.



9 July 1974 large quantities of rainwater were collected along with the hail, and on 18 August 1974 the catcher net was torn. Collected rainwater would melt the collected hailstones slightly, with the smaller hailstones the most affected. The torn catcher net should not have had any effect on the size distribution, since all sizes should have been more or less equally lost.

#### 4.3 Power Law Distributions

Some authors (Iribarne and de Pena, 1962; and Sulakvelidze, 1967) suggest that the size distribution of hail in a storm obeys a power law of the form:

$$C(D) = k D^{-\alpha} \quad (21)$$

where

$C(D)$  is the concentration per  $m^3$  in the diameter interval  $D-\delta D$  to  $D$

$D$  is the diameter of the hail in cm

$k$  and  $\alpha$  are constants.

This distribution is not a cumulative distribution like the previous ones, but a density function. Sulakvelidze has suggested a value of 3 for  $\alpha$ . Some values of  $k$  and  $\alpha$  for Equation 21 are given in the literature. Auer (1972) gives



$$C = 561.3 D^{-3.4} \quad (22)$$

for hail and graupel from a convective cloud system over the High Plains. Auer and Marwitz (1972) give

$$C = 616.5 D^{-3.5} \quad (23)$$

for hail and graupel in the air near a thunderstorm updraft.

Power law distributions were fitted to the calculated concentrations using a least squares method. The results are given in Table 9. The concentration for each size increment has been divided by the total concentration, so that  $k$  is less than 1. This procedure allows a comparison of the calculated variance to that for the other distributions.

The results indicate that the power law does not describe the storm samples very well, since the variance is about twice as large as for a log-normal distribution. Also, the slopes differ greatly from the Sulakvelidze value of 3. Figure 11 shows a log-log plot for the samples of 1974. On this graph, those hailstones with a diameter greater than about 1 cm match a distribution of the type

$$C = k D^{-3} \quad (24)$$



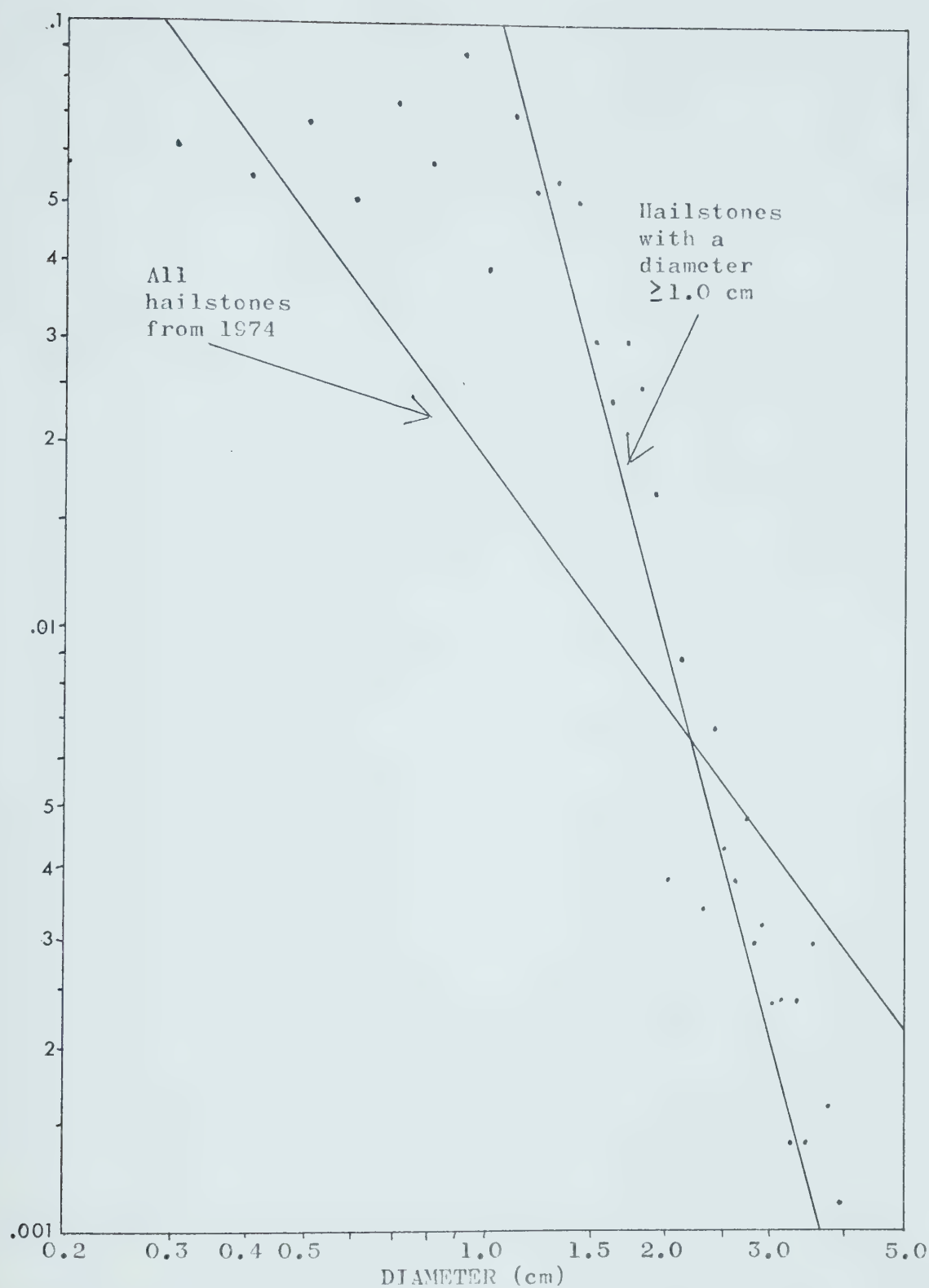


FIGURE 11. Power law size distribution of sequential hailstone samples from 1974. The two lines indicate the best-fitting distributions for all 1974 hailstones, and those greater than 1.0 cm respectively.



quite well. Apparently, the discrepancies from this distribution are caused by the smaller hailstones. Knowing this, the least squares were recalculated using subsets of the samples with some of the smaller hailstones eliminated. Table 9 shows the results of the calculations on these truncated samples.

These results are more encouraging. The slopes for the individual storms tend to be both larger and smaller than 3. The large "averaged" sample of 1974 has the slope closest to 3, suggesting that  $\alpha = 3$  is reasonable. In the cases where the smaller hailstones are neglected, the variance of the sample from a power law distribution is also reduced, as shown in Table 9.



SAMPLE DATE	ALL HAILSTONES			MINIMUM DIAMETER = 1.0 cm			MINIMUM DIAMETER = 1.5 cm		
	ALPHA	k	s <sup>2</sup>	ALPHA	k	s <sup>2</sup>	ALPHA	k	s <sup>2</sup>
1973	1.827	0.012	0.094	5.610	0.027	0.094	7.107	0.073	0.137
1974	1.333	0.019	0.180	5.716	0.115	0.070	4.013	0.159	0.071
23 July 1973	1.744	0.011	0.180	1.211	0.006	0.094	-	-	-
23 Aug 1973	1.736	0.012	0.090	1.614	0.009	0.029	-	-	-
27 Aug 1973	1.803	0.013	0.088	5.062	0.0292	0.073	-	-	-
24 Aug 1974	0.133	0.073	0.105	6.997	0.1351	0.062	-	-	-
2 July 1974	1.892	0.005	0.195	-	-	-	-	-	-
5 July 1974	1.641	0.011	0.383	5.149	0.006	0.049	-	-	-
9 July 1974	1.257	0.018	0.248	-	-	-	-	-	-
18 Aug 1974	0.342	0.0024	0.140	1.252	0.058	0.091	1.433	0.036	0.105
18 Aug 1974	0.998	0.039	0.195	4.091	0.193	0.085	6.042	0.832	0.054

TABLE 9.

Power law least squares fits for subsets of the concentrations of collected hailstones at the ground level. The two sets of figures to the right are for the truncated samples, from which hailstones smaller than MINIMUM DIAMETER have been excluded. The dashes indicate that the truncated sample contained no hailstones, hence no calculations were possible.



## CHAPTER 5. TIME-VARYING PROPERTIES

The detailed study of the time-varying properties of hailfalls will be based mainly on three storm sample sets. The storms were subjectively judged to be of different severities, based on the criteria of hail amount, hail size, duration of hailfall, and whether rain was falling with the hail. The presence of rain during a hailfall may indicate that some of the small hail produced by the storm melted before reaching the ground. The three storms selected occurred on 9 July 1974, a "weak" storm; 24 June 1974, a "moderate" storm; and 18 August 1974, a "severe" storm. The information for other storm samples is included in Appendices 3 and 5.

### 5.1 Variation of Size Distributions with Time

Since hailstones of differing size generally have different terminal velocities, the measured values of number flux and concentration in the air at ground level are not the same as those aloft. In addition, vertical shear of the horizontal wind will cause horizontal sorting of hailstones according to size. For a stationary storm, if all the hailstones originated at one point and one time, the largest hailstones would reach the ground first, followed by the smaller ones. If the production of the hail continues with no change in the initial spectrum, then eventually the hail size distribution between the storm and the ground will



become homogeneous. If this storm now moves over a point on the ground, the initial hail collected at this point will consist partially of small hail as well as the large hail collected in the case of a stationary storm. Thus, the sequential samples for a moving storm may have an excess of small hailstones at the first of the sampling period compared to the sequential samples from a stationary storm. This result could be modified if different assumptions about the hailstone distribution within the storm are made.

Figures 12, 13 and 14 show the hailstone size spectra at ground level as a function of time for each of the three storms. Using these, an attempt was made to detect the sorting of the hail by size. The hailfall of 9 July 1974 (Figure 12) at the sampling site consisted of two events. The hailfall began with a fairly narrow size spectrum in the first two minutes, which broadened in the next two minutes. The hail had almost ceased by the third sample, from five to six minutes. In the fourth sample interval, from seven to eight minutes, the hail had started again, with another narrow spectrum. It then diminished in intensity for the final time, while the spectrum remained quite narrow.

The hail concentration of 24 June 1974 (Figure 13) was continuously decreasing in each sampling period. The beginning of the hailfall was not collected, which may explain the absence of a period of increasing hail concentration. The first sample had the broadest range of sizes, as well as the greatest concentration. The largest hailstones, those greater than about 1.0 cm in diameter, ceased falling the soonest, disappearing largely after the first sample interval. The smallest hail re-



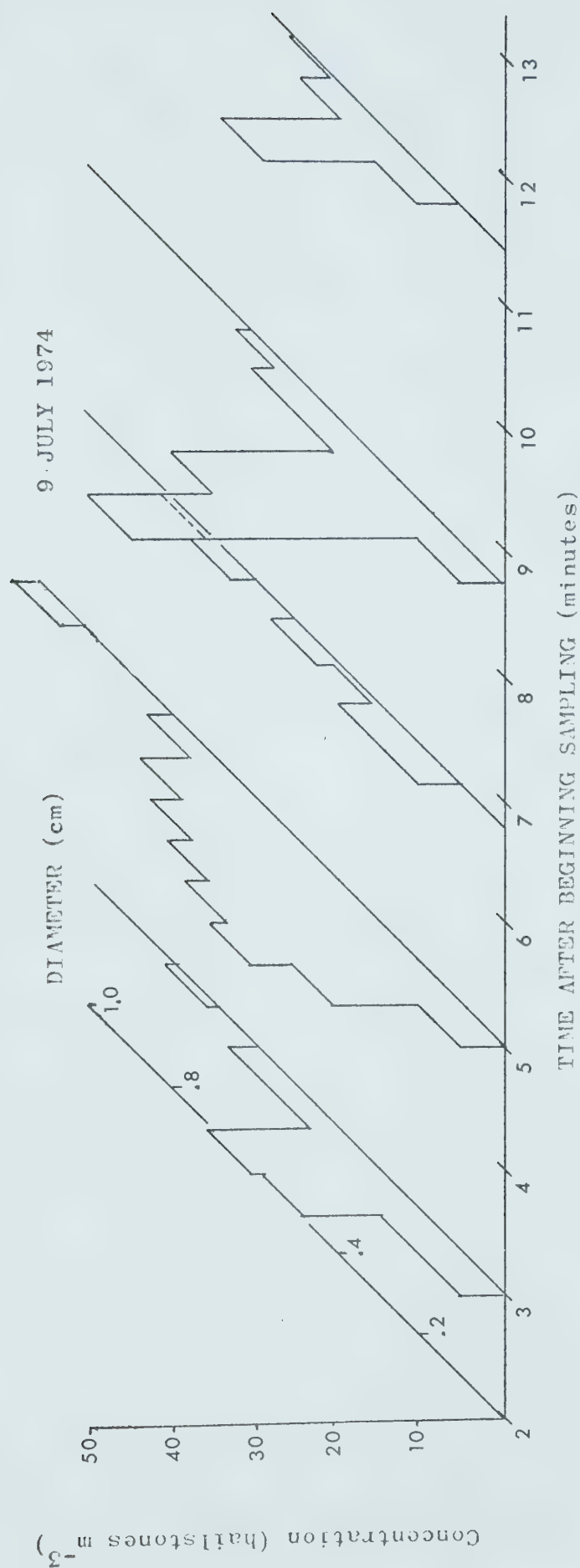


FIGURE 12. Hailstone concentration vs time and diameter. Each curve represents one sample and is located in time at the midpoint of the sampling interval. The first collected sample has been omitted because it contained no hailstones.



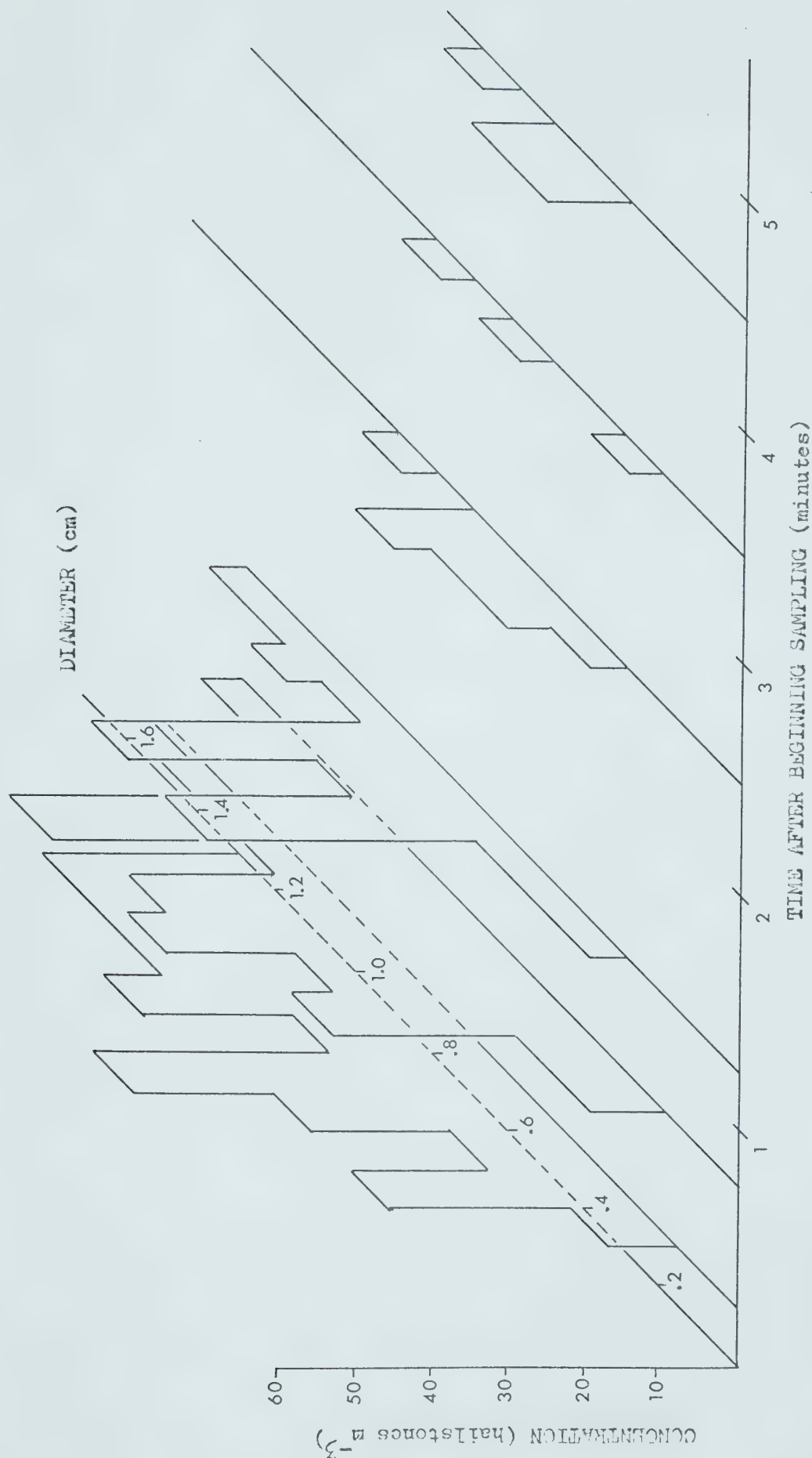


FIGURE 13. Hailstone concentration vs time and diameter. Each curve represents one sample and is located at the midpoint of the sampling interval.



mained the most constant in concentration throughout the sampling period. Because of the lesser requirements of updrafts and liquid water required for its growth, small hail can be expected to have a greater area of origin.

The hailfall of 18 August 1974 is shown in Figure 14. In this storm, the hailfall began with hail smaller than 1.0 cm. There was an abrupt drop in the concentration of the small hail as the larger (up to 2.0 cm) hailstones began to arrive. The largest hail came during the period from 9 minutes 20 seconds to 10 minutes, which almost coincides with the greatest concentration of all hail. The smallest and largest hail stopped falling between 10 minutes and 10 minutes 20 seconds, with the intermediate sizes continuing to the end of the shower with a reduced concentration.

Of the three storm samples, the one of 18 August 1974 showed the greatest evidence of hail size sorting by the horizontal wind. The storm moved quite rapidly, with a speed of about  $10 \text{ m s}^{-1}$ . The storm of 24 June 1974 had a similar velocity, but the absence in the record of the first part of the hailfall makes it impossible to know whether there was an abundance of small hail in it also.

## 5.2 Variation of Other Parameters with Time

The onset time of hailfall at the collecting sites was estimated from the tape transcripts.



18 AUGUST 1974

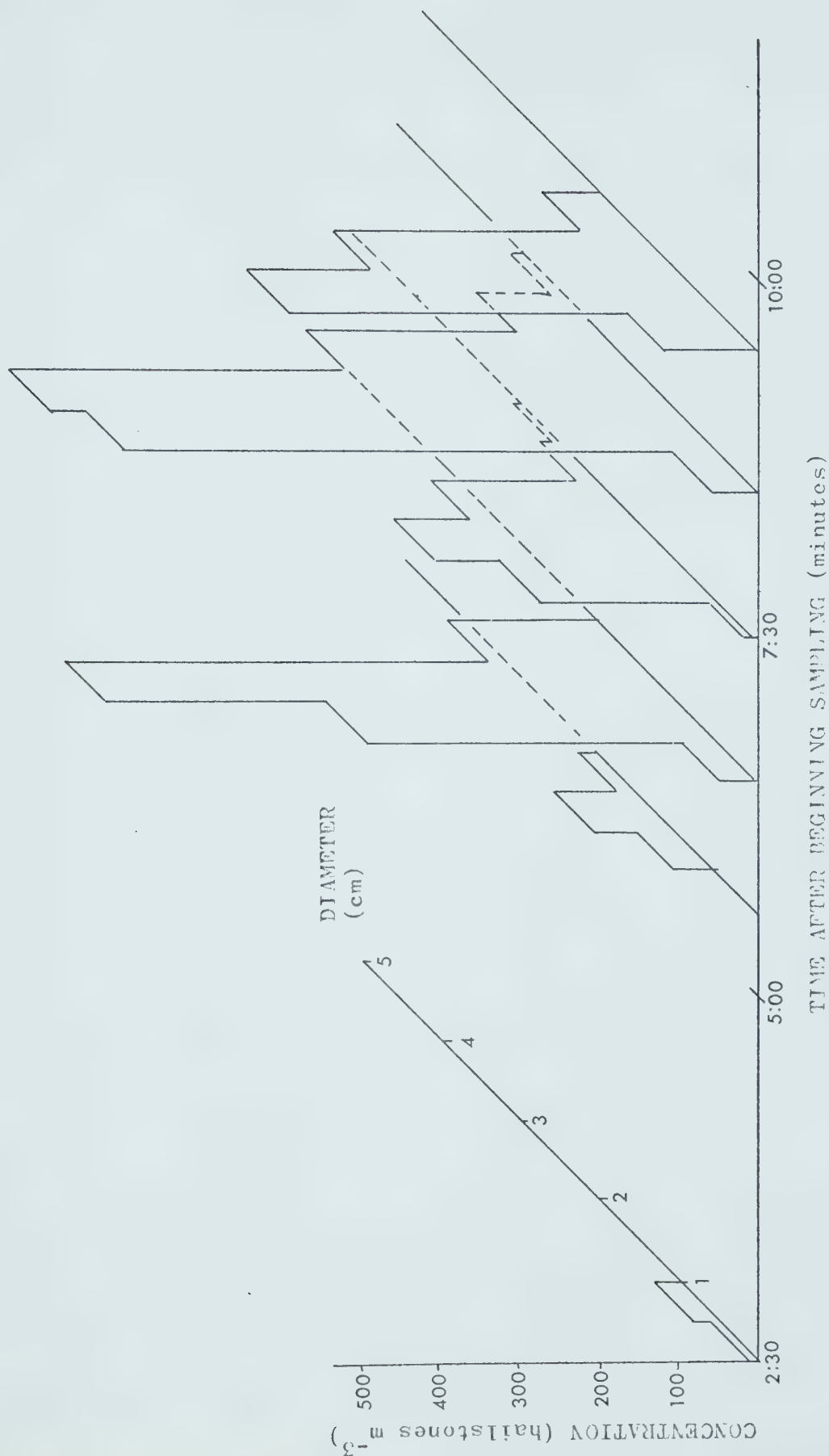


FIGURE 14. Hailstone concentration vs time and diameter. Each curve represents one sample and is located at the midpoint of the sampling interval. The last two samples had very low concentrations and have therefore been omitted.



1. On 9 July 1974 the hail began approximately 2 minutes after beginning sampling. During the first 2 minutes of sampling, rain was falling.
2. On 24 June 1974 the hailfall began 1.5 minutes before sampling was started.
3. On 18 August 1974 the hailfall began at the same time as the sampling.

The samples were not of the same duration because the usual practice was to collect a sample sufficient to fill most of a sample container. The sampling intervals were therefore adjusted according to the rate of precipitation.

The errors indicated by the error bars in the following graphs come from three sources.

1. There is a possible 1 percent error in the measurement of the effective area of the hail catcher aperture. It is felt that losses due to bouncing and through the mesh holes probably contributed at most 5 percent error in the number.
2. Timing errors were introduced by approximate switching times and inaccurate clocks. For short samples of a duration of about 15 seconds, the maximum error is about 5 percent.
3. Errors in measuring the sizes and numbers of hailstones varied with the quality of the sample. These uncertainties ranged from greater than 100 percent for some of the samples of 9 July 1974 to 5 percent for some samples from 18 August 1974. These values were derived from repeated analyses of the same samples.



The time variation of hailfall flux density (number of hailstones per unit area per unit time) is shown in Figure 15.

The following features can be seen:

1. The point duration of hailfall varied from 6 minutes to 17.5 minutes. All of these values are less than the modal value of about 20 minutes reported by Pell (1971). Pell's value came from hailcard information. Although the small number of hailstorms considered here is probably not a significant sample, the present results suggest that one should investigate the possibility that hailfall durations are over-estimated on hailcards.
2. The hailfall occurs in bursts. Two bursts, at about 5 minutes and 10 minutes after the beginning of sampling are quite prominent on 9 July 1974.
3. The number flux of the hailfall may vary by a factor of ten during the time of "heavy" hailfall. Heavy hailfall here refers to number fluxes greater than  $10 \text{ m}^{-2} \text{ min}^{-1}$ .

Figure 16 shows the mass flux of ice as a function of time. Results for the storm of 9 July 1974 are not included, because the large amounts of collected rainwater obscured the mass measurements. The maxima and minima occur at the same times as those in Figure 15, but the relative maxima and minima are not as extreme as those for the number flux variations. Since the size distribution is such that the number of hailstones decreases as their diameter or mass increases, the greatest contributions to variations in number flux will come from small hailstones, which



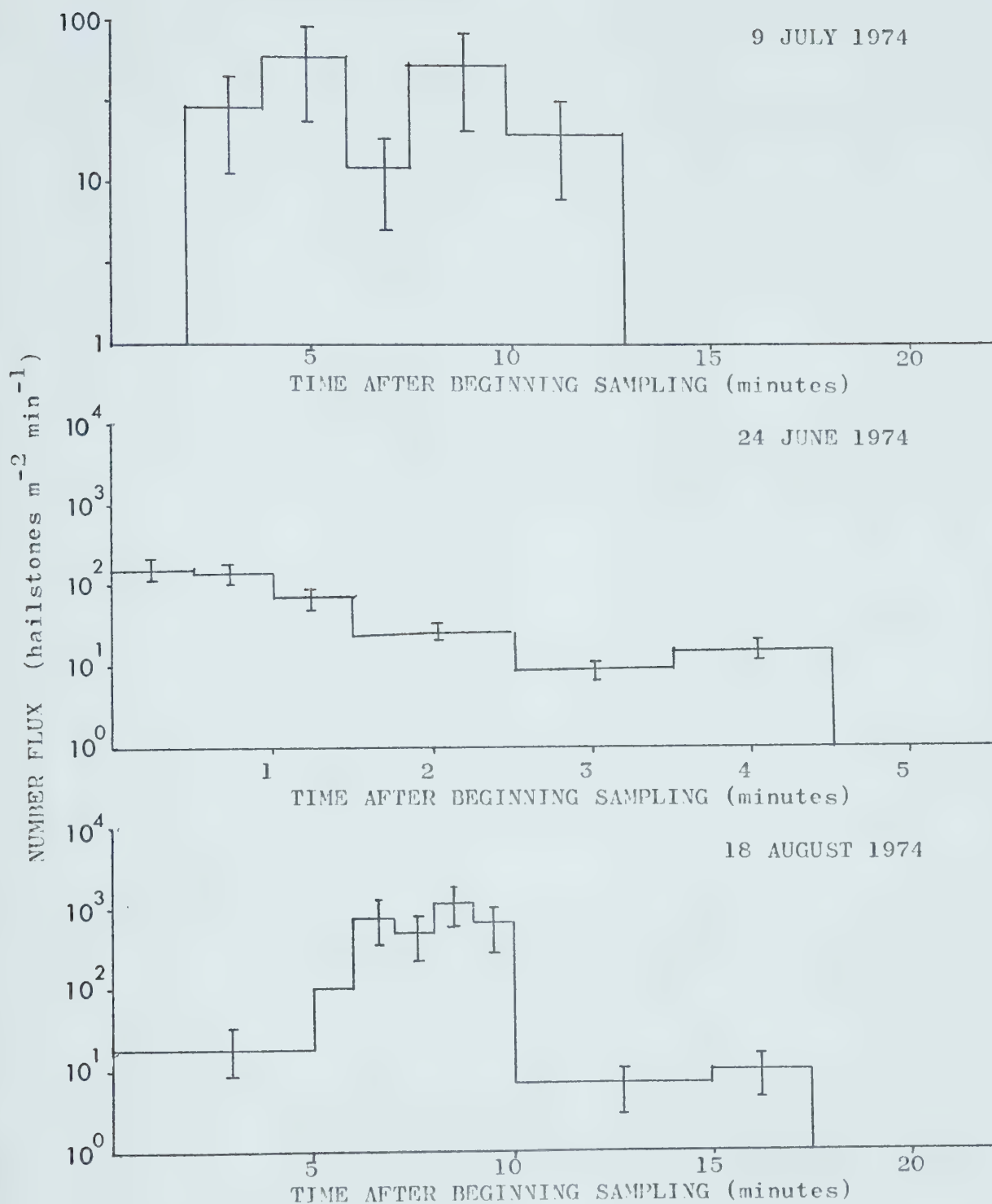


FIGURE 15. Number flux as a function of time. Each horizontal bar represents the number of hailstones collected  $\text{m}^{-2} \text{min}^{-1}$ . The error bars represent errors in timing, collection area and counting.



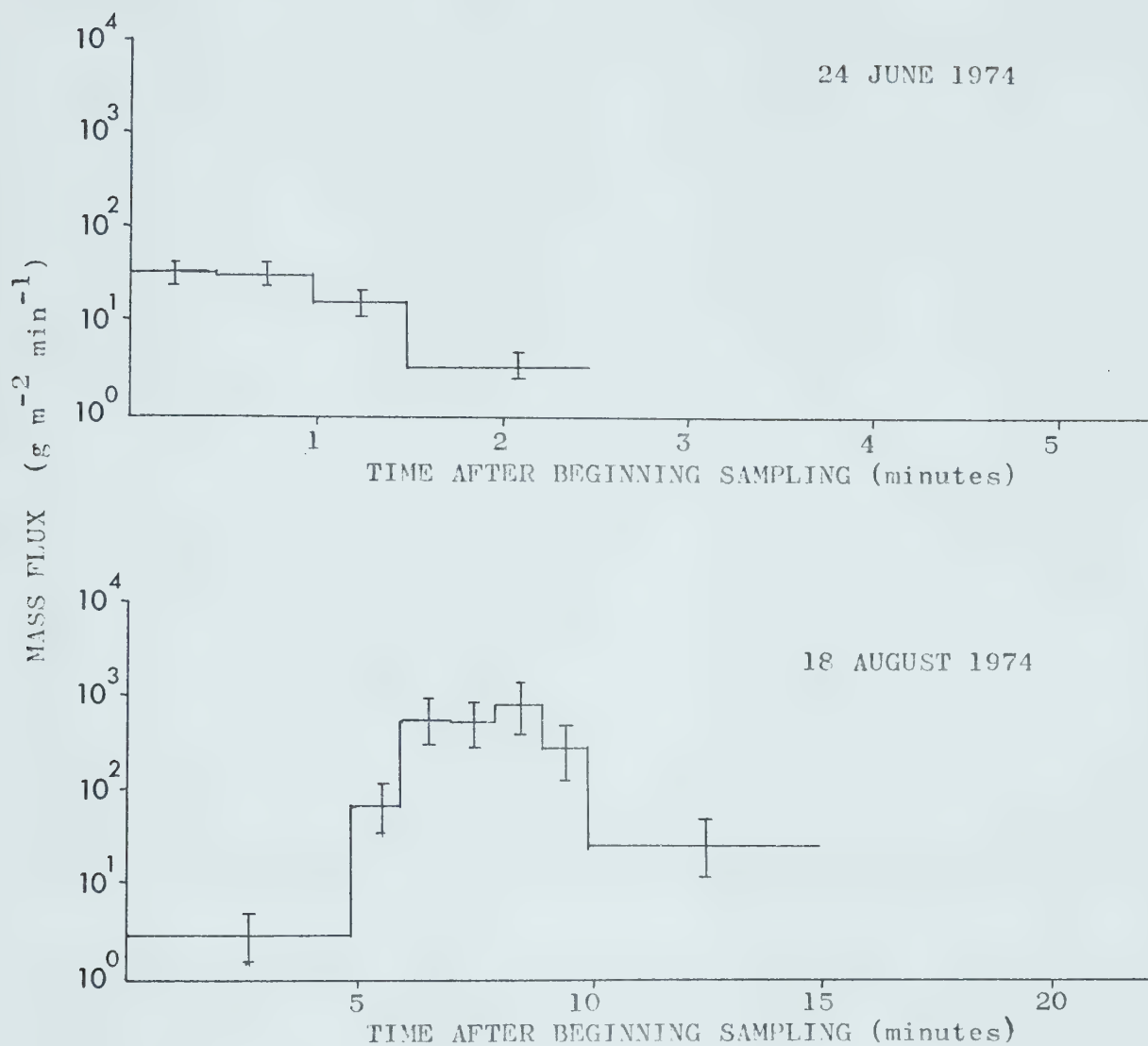


FIGURE 16. Mass flux as a function of time. The open ends of the graphs indicate that the subsequent samples were so small that contamination by collected rainwater made mass measurements invalid.



will cause smaller changes in mass flux.

Figure 17 shows the variation of the mean and median diameters of the samples with time. The variation of the two parameters is similar. The mean diameter increases to a maximum during the hailfall, then decreases. To see whether these peaks correspond to those of number flux, the two variables, number flux and mean diameter, were correlated and the results are given in Table 10.

---

<u>DATE OF SAMPLE</u>	<u>R</u>
9 July 1974	-0.24
24 June 1974	0.59
18 August 1974	0.03

---

TABLE 10. Correlation coefficient R between number flux and mean diameter for three sets of storm samples.

There is no evident correlation between the number flux and mean hailstone diameter from these three examples. A qualitative comparison of the two graphs (Figures 15 and 17) reveals that the greatest discrepancies between the two variables occurs at the end of the hailfall, when the number fluxes are small. The first 1.5 minutes of hailfall on 24 June 1974 were not collected, so the high correlation in that case may indicate that the two variables correlate well during the more intense middle portions of a hailfall.

The hypothesis that the number flux is correlated with the maximum hailstone diameter of a sample was also tested. The



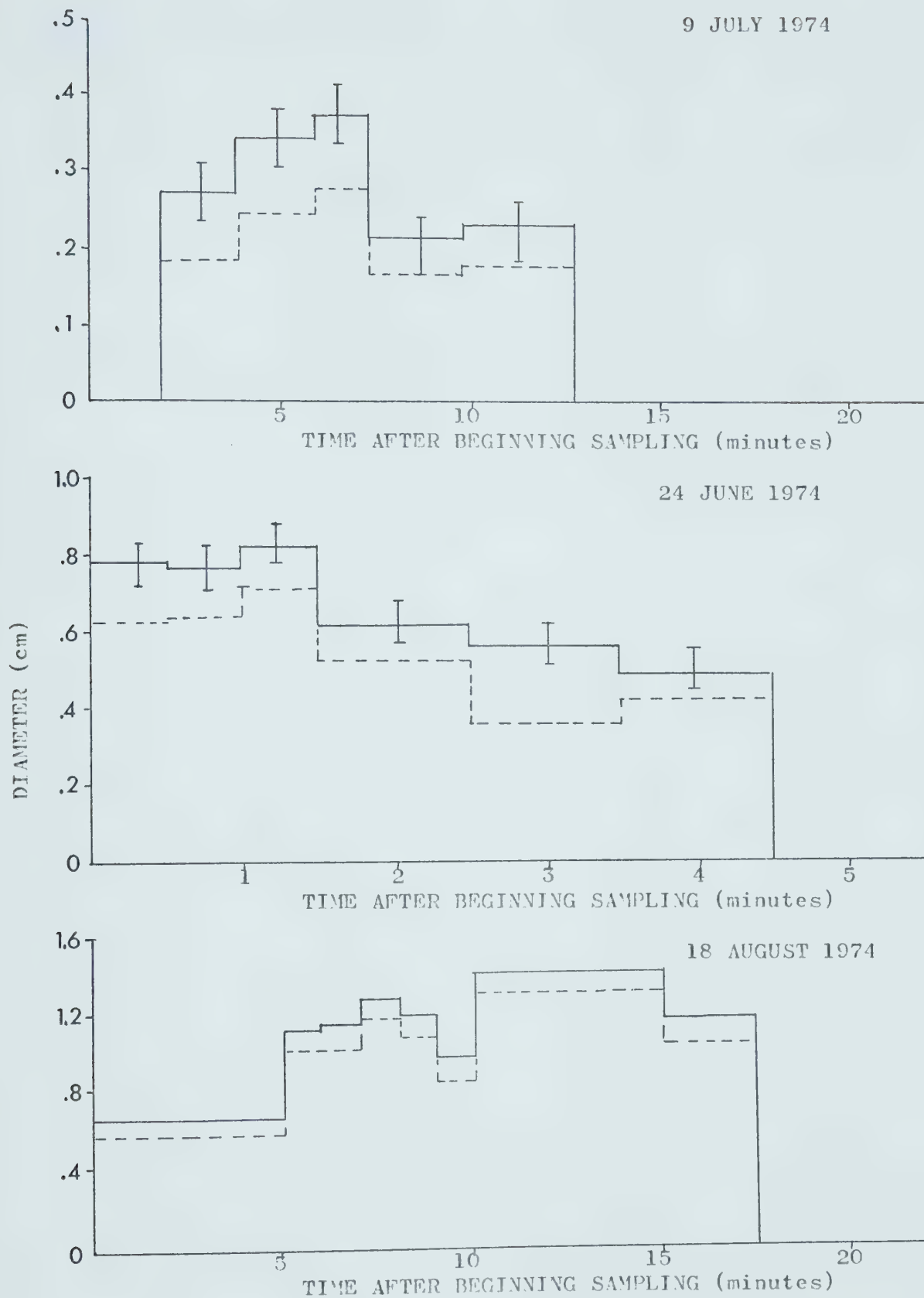


FIGURE 17. Mean and median diameter vs time. The solid line indicates mean diameter. The dashed line indicates median diameter.



results are given in Table 11.

---

<u>DATE OF SAMPLE</u>	<u>R</u>
9 July 1974	0.88
24 June 1974	0.70
18 August 1974	0.71

---

TABLE 11 Correlation coefficient R between number flux and maximum diameter for three sets of storm samples.

These results indicate a favorable correlation, suggesting that the conditions for large hail may be related to those for large quantities of hail.

Figure 18 shows the change in the variance of the number flux with time. Since the variance is defined here to be a measure of the deviation of the sample distribution from an exponential distribution, a low variance indicates that the hail-fall is approaching an exponential distribution. The graphs show a variance minimum at the times of the number flux maximum. If reductions in number flux are due in part to dispersion of hailstones by the winds below a storm cell, then periods of greater number flux would correspond to storm samples less disturbed from the actual distribution within the storm. If the size distribution of hail within the hailstorm is exponential, then the variance of the distribution at the ground would be smaller for greater number flux, as observed.

Figure 19 shows the variation with time of hailstone concentration, given by Equation 17. The features of the graph are similar to those of Figure 15, but the maxima and minima



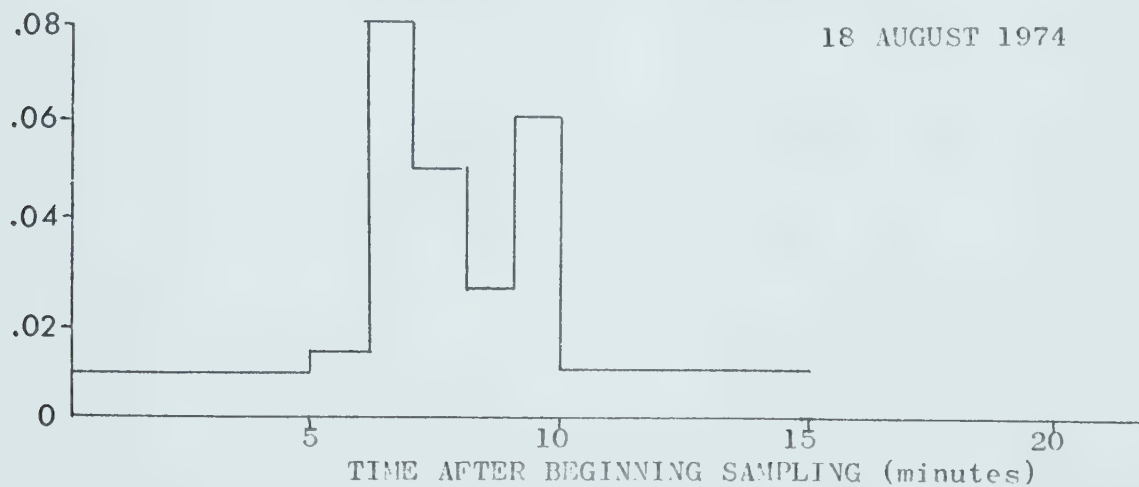
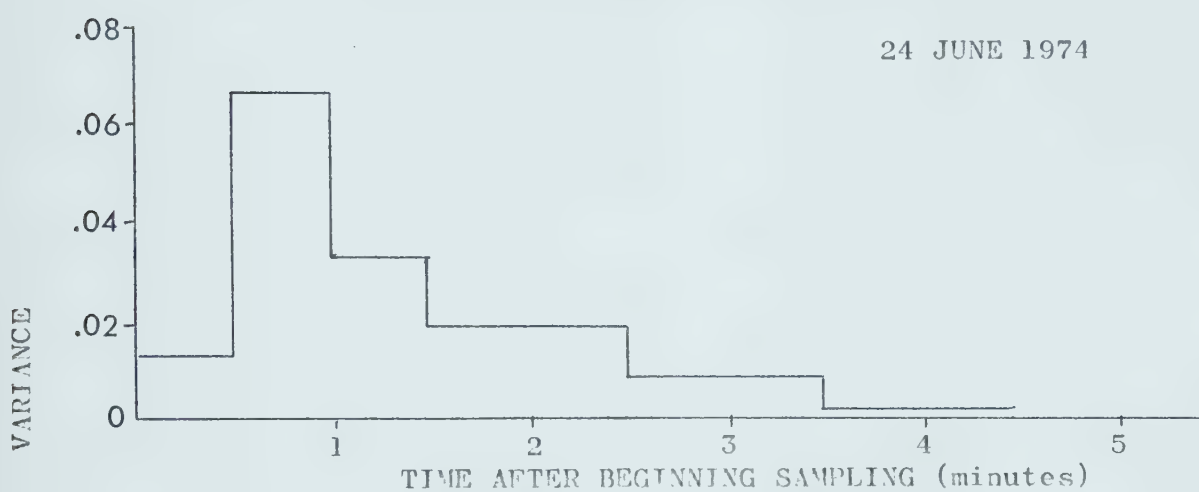
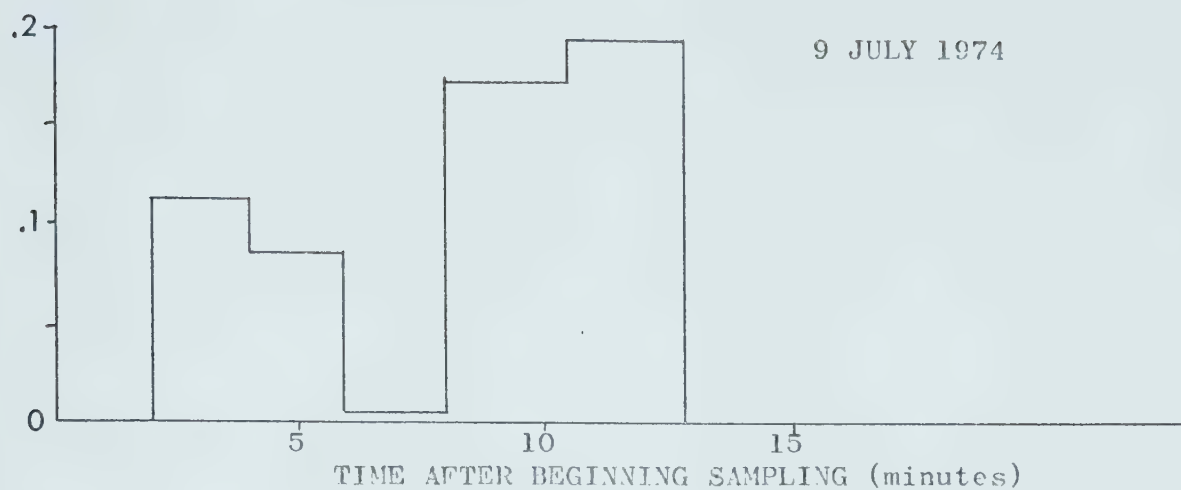


FIGURE 18. Variance of sample distributions from an exponential distribution. Open ends of the graphs indicate a sample too small to compute the variance (fewer than two hailstones).



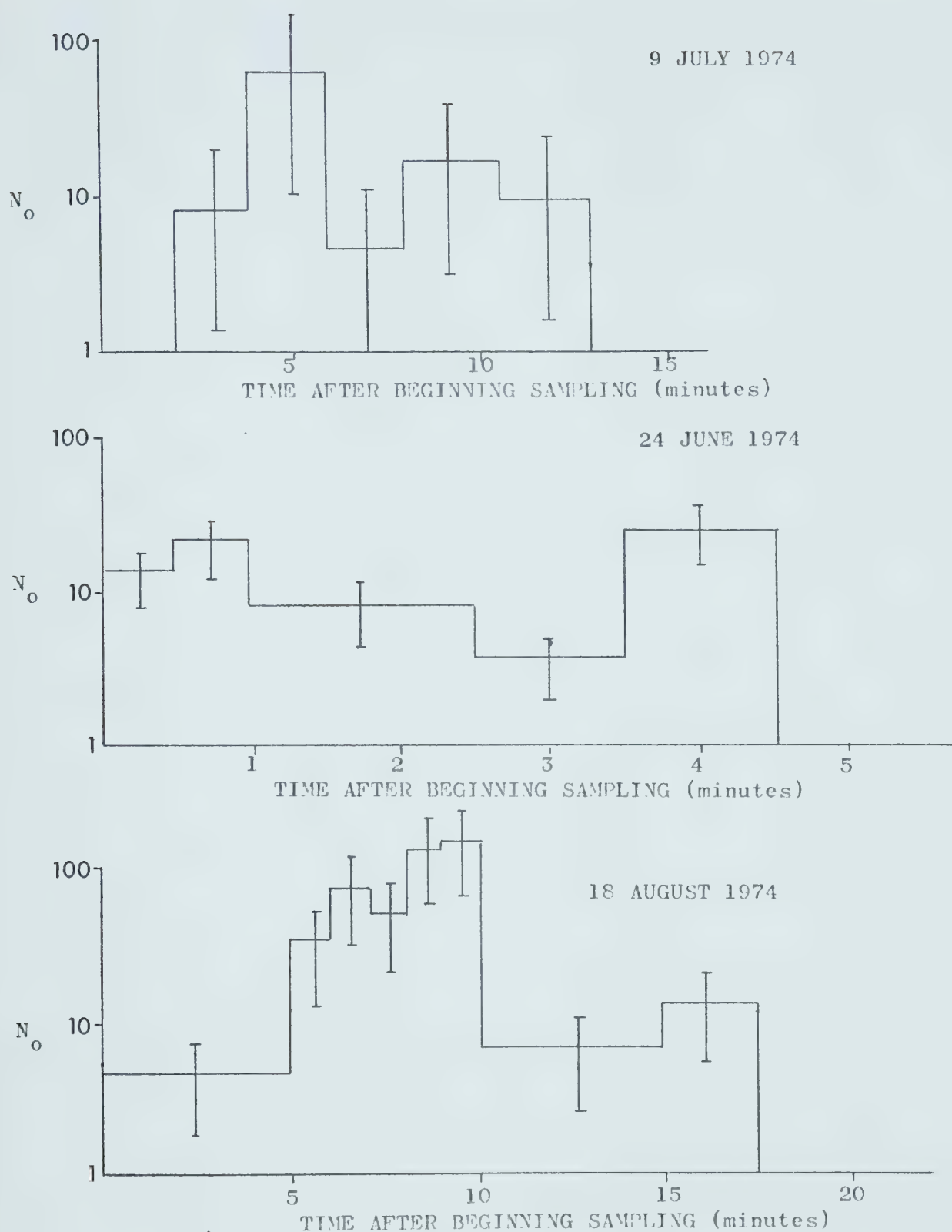


FIGURE 19.  $N_o$  of the best-fitting exponential distribution for concentration measurements. The error bars indicate accumulated errors in collection and analysis.



are more prominent. This is a consequence of the concentration being a function of the terminal velocity of the hailstones. Douglas (1964) gives  $N_0 = 32.2 \text{ m}^{-3} \text{ cm}^{-1}$  for his exponential distribution for 67 hail samples collected from 1958 to 1964. For small samples, the present results show that  $N_0$  can vary either way by up to a factor of ten.

Ulbrich (1974) derived the two parameters,  $\Lambda$  and  $N_0$ , of an assumed exponential distribution along with the maximum diameter from the Doppler radar spectrum of falling hail. His use of a vertically pointing radar implied a sampling volume extending over the entire depth of the storm. Figure 20 shows the temporal changes of these parameters in a hailstorm on 10 August 1966.

$\Lambda$  and  $N_0$  decrease with time, while the maximum diameter increases. Some of the values given for  $\Lambda$  and  $N_0$  are considerably larger than those found in the present work and in the literature (Douglas, 1964; and Atlas, 1963). This discrepancy seems to be caused by the rain also measured in the Doppler spectrum. Ulbrich states that the total hailstone concentration for all sizes decreases from  $1000 \text{ m}^{-3}$  to  $10 \text{ m}^{-3}$  and the median diameter increases from about 0.1 cm to 1.0 cm during the period of observation from 1502:39 to 1511:00. With regard to  $\Lambda$  and  $N_0$ , he says "...the temporal behavior of  $N_0$  and  $\Lambda$  implies a size distribution which gradually broadens to hailstones of larger diameter and for which the number of smaller diameter stones is decreasing."

Another time variation study of the parameters  $N_0$  and  $\Lambda$  was performed by Federer and Waldvogel (1975) for a hailstorm in



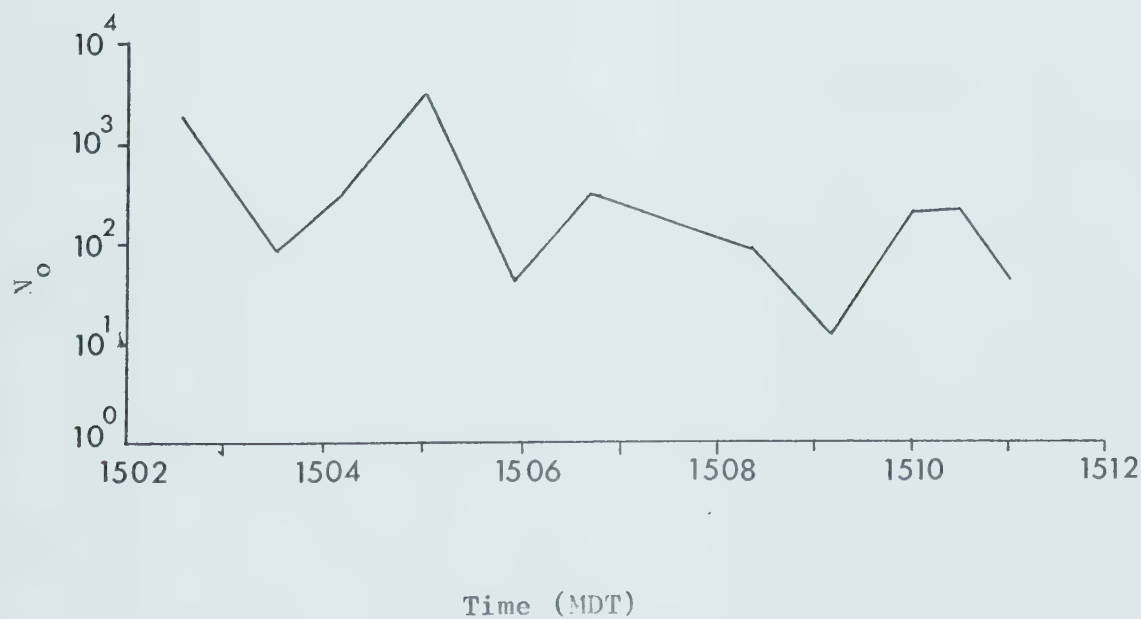
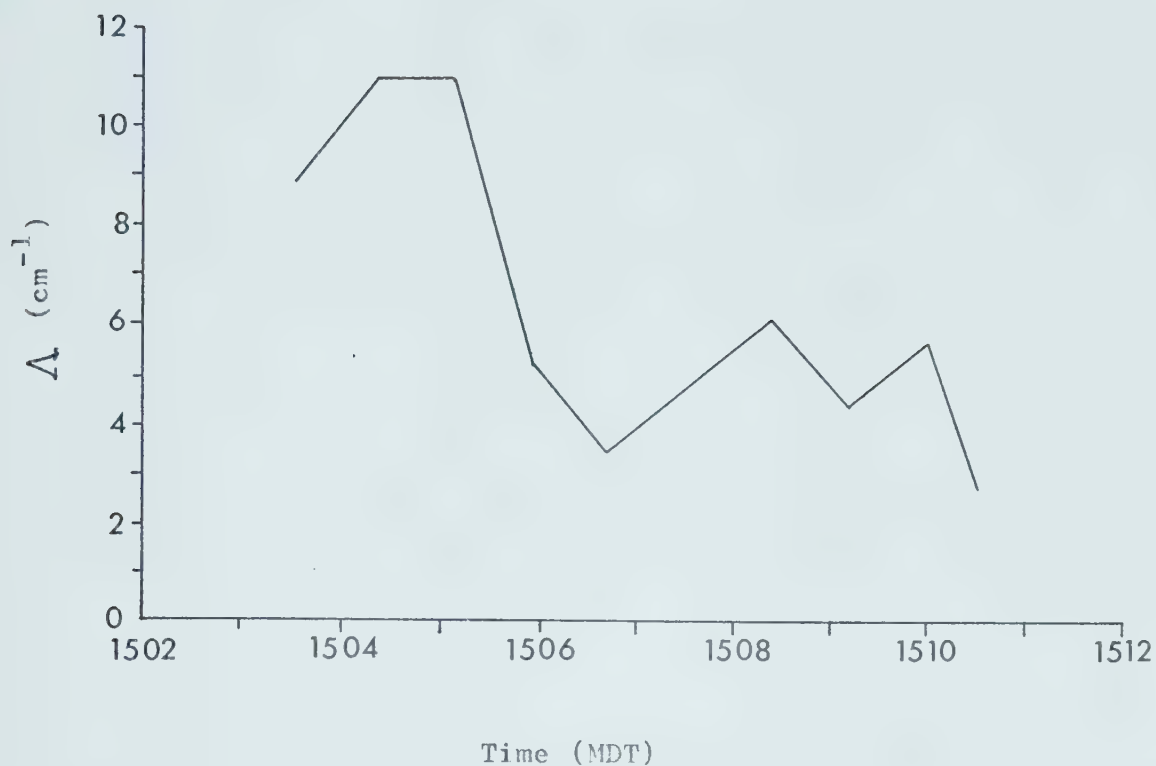


FIGURE 20 Change with time of  $\Delta$  and  $N_o$  in a hailstorm as observed by Doppler radar. (From Ulbrich, 1974)



Switzerland on 6 July 1973. They interpreted their results to show the passage of 4 different hail cells, each lasting for 2 to 3 minutes. At the beginning of each cell, mainly large hailstones were found, and smaller hailstones at the end of the passage of each hail cell. In that storm, the number flux and median diameter did not increase simultaneously toward the center of the hailfall, contrasted with the results of this study in Figures 15 and 17. Their results indicate that  $\Lambda$  showed an increasing trend during the passage of the four hail cells.

### 5.3 Statistical Significance

Joss and Waldvogel (1969) estimated the sample size required to make a good estimate of the parameters of an exponential distribution of precipitation particles. Their study applied to three cases of rainfall — drizzle, widespread rain, and thunderstorm rain. They determined the product of the sampling area  $A$  and the sampling time  $t$  that was required to approximate either the precipitation rate  $R$  or the radar reflectivity  $Z$  to the desired accuracy. As an example, to find an  $R$  or  $Z$  value with a probability of 95 percent which deviates less than 10 percent from the mean value, assuming a widespread rain of  $1 \text{ mm hour}^{-1}$ , the product  $At$  had to be at least  $1.5 \text{ m}^2\text{s}$ .

Their technique was adapted to hail, using precipitation rates from  $1.0$  to  $100.0 \text{ mm hr}^{-1}$ , which correspond to mass fluxes



of 17 to 1700 g m<sup>-2</sup> min<sup>-1</sup>. The worst case sample in this work is approximately a 10 second sample over an area of 0.58 m<sup>2</sup> in a precipitation rate of 1 mm hr<sup>-1</sup>. For this sampling case, the exponential distribution parameters estimated from the sample would be within 5 percent of the mean value 95 percent of the time. Other samples should give even better estimates. The conclusion is that, according to the Joss and Waldvogel criterion, the sampling times used in this experiment are long enough to give useful estimates of distribution parameters.



## CHAPTER 6. HAILSHAFT MODELLING

If the concentration size spectrum of hail at the ground is known as a function of time, the concentration which occurred at upper levels can then be inferred by extrapolating backwards in time. The upper concentrations will be modified by horizontal and vertical winds, changing air density, and growth or melting of the hailstones, as well as by the differential motions of hailstones of varying sizes with respect to the air.

A simple two-dimensional model was developed to determine the previous concentrations of the hail samples . The model used the hail concentrations at the ground calculated from the sequential samples using Equation 17. The upper air concentrations can be evaluated completely only if the ground concentrations are known for many points. Several assumptions were made to simplify the treatment of the modifying processes mentioned above.

The hailstones were assumed neither to grow nor to melt. This assumption is not entirely unreasonable since there can be no growth below the freezing level, and, for hailstones with a radius greater than about 0.5 cm, melting will not be significant.



The hailstones were assumed to fall at their terminal velocity relative to the air. The terminal velocity is estimated by Equation 18. The air density was determined from the hydrostatic equation and the ideal gas equation, assuming a constant lapse rate:

$$\rho_A(Z) = \frac{\rho_s (T_s - \Gamma Z)^{\frac{g}{\Gamma R} - 1}}{R T_s \frac{g}{\Gamma R}} \quad (25)$$

where

$\rho_A(z)$  is the air density at  $z$

$\rho_s$  is the air density at the surface

$T_s$  is the air temperature at the surface

$\Gamma$  is the lapse rate

$Z$  is the altitude above the surface

$g$  is the acceleration of gravity

$R$  is the specific gas constant for dry air.

The following values were used in the model:  $T_s = 20^\circ\text{C}$ ,  $\Gamma = 6.5 \text{ K km}^{-1}$ ,  $g = 980.6 \text{ cm s}^{-2}$ ,  $\rho_s = 1.05 \times 10^{-3} \text{ g cm}^{-3}$ . Using these values, the freezing level occurs at about 3.1 km above the surface.

Let the concentration of hailstones with diameter  $D$  at an altitude  $z$  at a horizontal distance from the sampling site  $x$  be  $C(D, x, z, t)$ . The collected samples correspond to  $C(D, 0, 0, t_s)$ , where  $t_s$  is the sample time. The model then calculates  $C(D, x, z, t)$  for other values of  $x$ ,  $z$ , and  $t$ .



The model begins with the hailstone concentration for the smallest diameter interval calculated from the last sample near the ground —  $C(D_i, x_i, z_i, t_f)$ ,

where

$$D_i = 0.5 \text{ cm}$$

$$x_i = 0$$

$$z_i = 0$$

$$t_f = \text{the midpoint of the last minute of sampling.}$$

At the collection site the atmosphere is described by

$$T_s = \text{the surface temperature}$$

$$P_s = \text{the surface pressure}$$

$$\rho_s = \text{the surface air density. The upper air conditions}$$

are then calculated by Equation 25. This knowledge of upper

air conditions allows the calculation of the terminal velocity

of a falling hailstone at an altitude  $z$  using Equation 18. A

fixed time step of 1 minute is used to extrapolate the concen-

trations backward in time and space in a Lagrangian fashion.

This time step was chosen to correspond to the sampling interval

used for most of the collected samples. Vectors representing the

movement of a hailstone with diameter  $D$  at an altitude  $z$  were

computed in the following ways. In the horizontal, the hailstone

was assumed to move with the air velocity with respect to the

ground. Hence the horizontal speed of any hailstone is given by

$$V_H(Z) = \alpha Z \quad (26)$$

where  $\alpha$  is the wind shear. The form of  $\alpha$  is given in Figure 21.



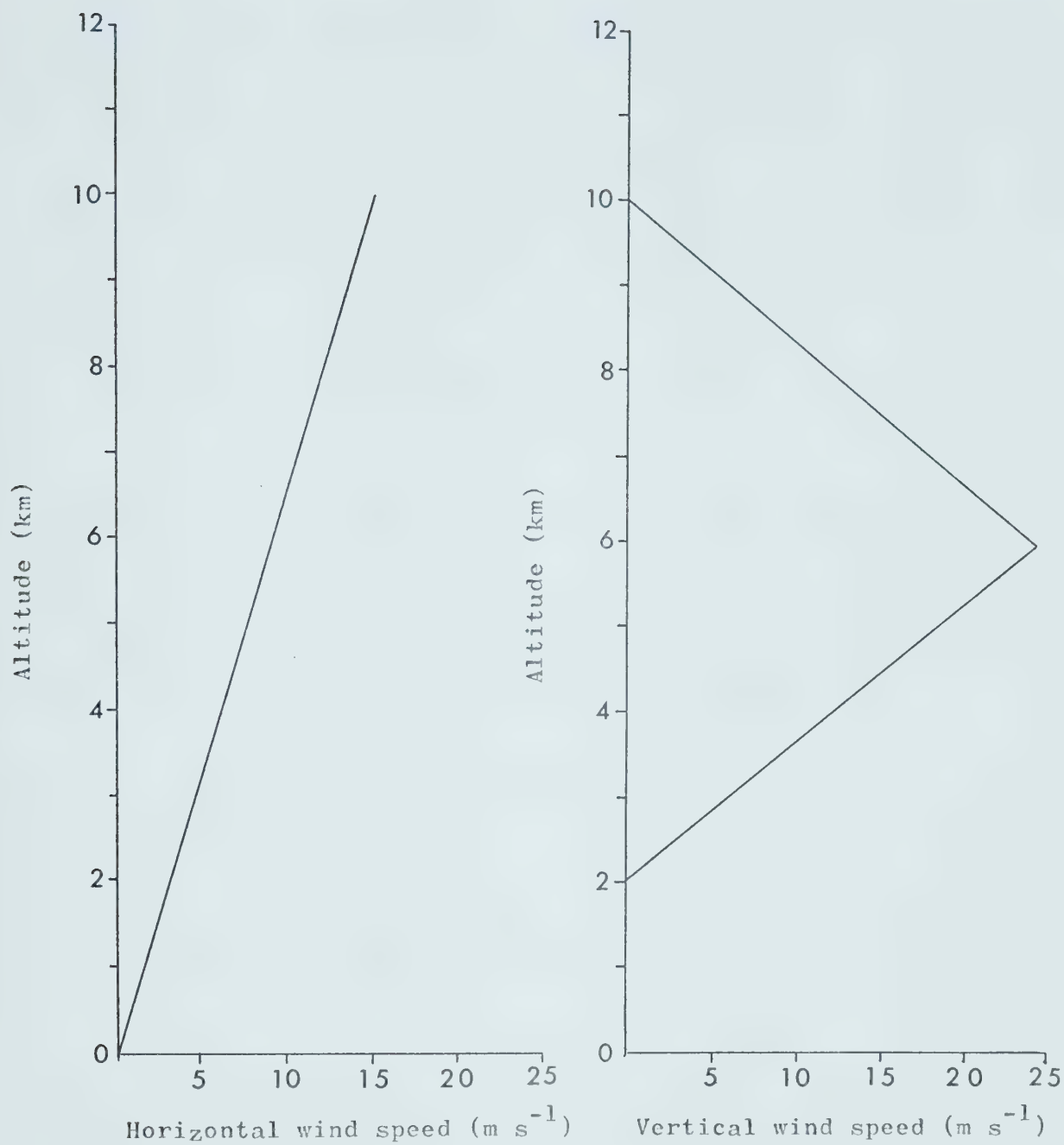


FIGURE 21. Wind shear and updraft profiles for the hailfall model.



In the vertical direction, the hailstones were assumed to fall with their terminal velocity with respect to the air. The assumed updraft profile is shown in Figure 21, with the maximum updraft velocity approximately equal to the terminal velocity of the largest collected hailstone. Then the vertical velocity of a hailstone with respect to the ground is given by

$$V_v(z) = V_T(D, z) - V_u(z) \quad (27)$$

where  $V_u(z)$  is the updraft velocity at  $z$ .  $V_v(z)$  will be negative for hailstones falling with respect to the ground. Then during a small time step  $\delta t$  near an altitude  $z$ , a hailstone with diameter  $D$  will be displaced the following distances:

$$\delta z = V_v(D, z) \delta t \quad (28)$$

$$\delta x = V_h(D, z) \delta t$$

Then if the concentration at one point  $C(D, x, z, t)$  is known, the concentration at another point at an earlier time,  $t - \delta t$ , can be determined by

$$C(D, x - \delta x, z + \delta z, t - \delta t) = C(D, x, z, t) \cdot \frac{V_v(z)}{V_v(z + \delta z)} \quad (29)$$

This equation was evaluated at a grid of points separated by



thirty 100 m intervals in the horizontal, and fifty 200 m intervals in the vertical.

The updraft profile and the wind shear are approximations to the conditions which could have prevailed on 18 August 1974 at the sampling site and time. The wind shear was approximated from the storm velocity at 10,000 m as observed by the ALMAP radar. The updraft profile was made symmetrical, with a maximum velocity approximately equal to the terminal velocity of the largest collected hailstone. Both the wind shear and the updraft velocity profile would have been more complicated in the real storm. The sample hailstones were grouped into size categories 0.5 cm wide and all the hailstones within a size category were assumed to fall with the terminal velocity of a sphere with the average diameter for that category. The computed concentrations for the 12 minutes of model time are shown in Figure 22. The concentrations were computed backwards in time, so that the cumulative errors are greatest for the first minute, and decrease as time progresses. The sampling site is in the lower right hand corner. All times are MDT.

The model is limited in that the concentrations calculated represent only hail that fell at the sampling site. Other hailstones may be at the same point in space and time, but, if they have different sizes, they will fall elsewhere.

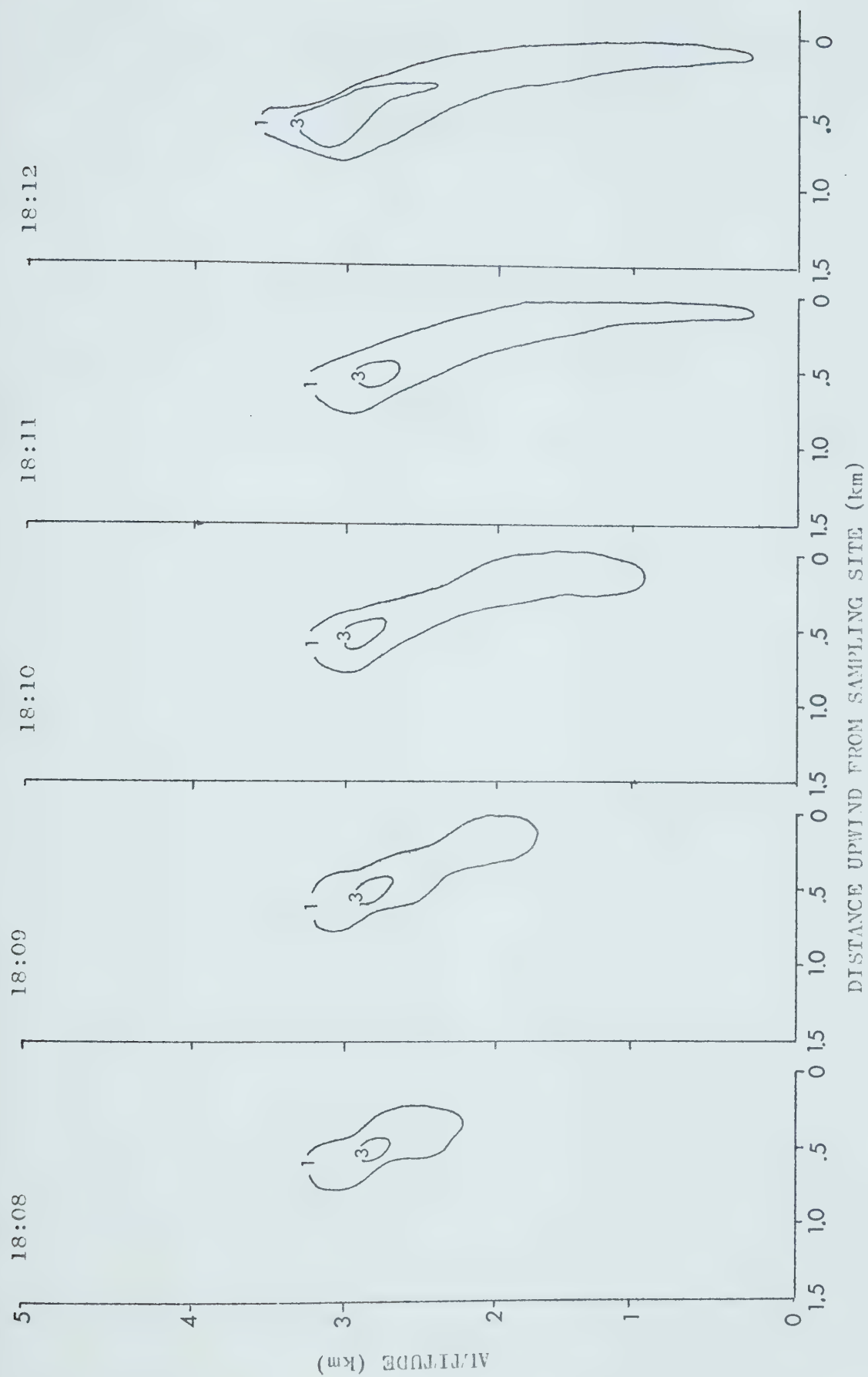
One feature of the results is the two separate areas of concentration maxima at 18:15 and 18:16. The upper region would consist of hailstones that are partially supported by the updraft. They first move into the area depicted in Figure 22 at about the level of the updraft maximum and fall with a velocity of  $3 \text{ m s}^{-1}$



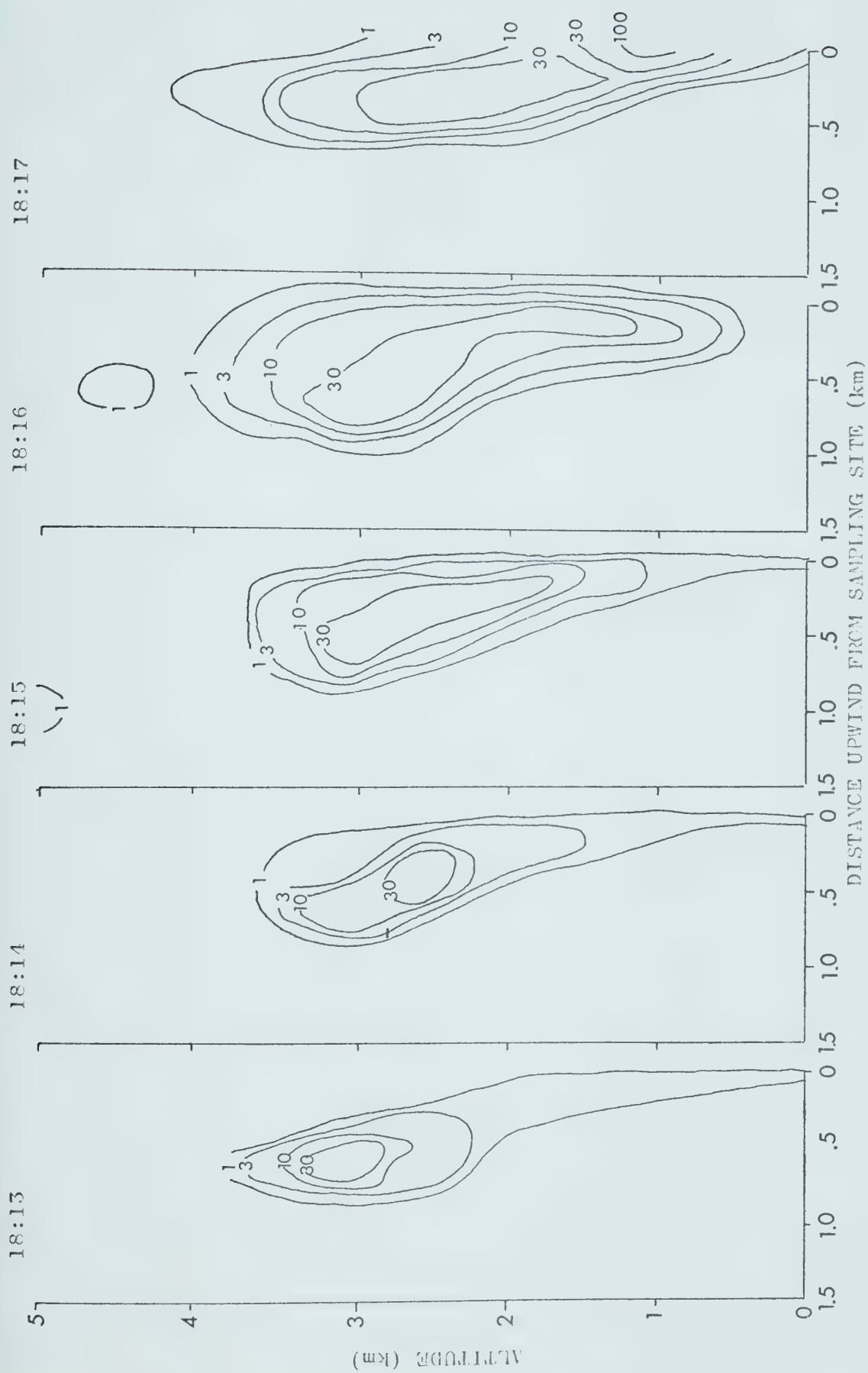
FIGURE 22.

Isolines of hailstone concentration produced by the hailfall model above and upstream of a hail sampling site. The samples used in the model were collected on 18 August 1974 beginning at 18:10 MDT. The isolines are at approximately logarithmic intervals and enclose areas of concentration in hailstones  $\text{m}^{-3}$ .

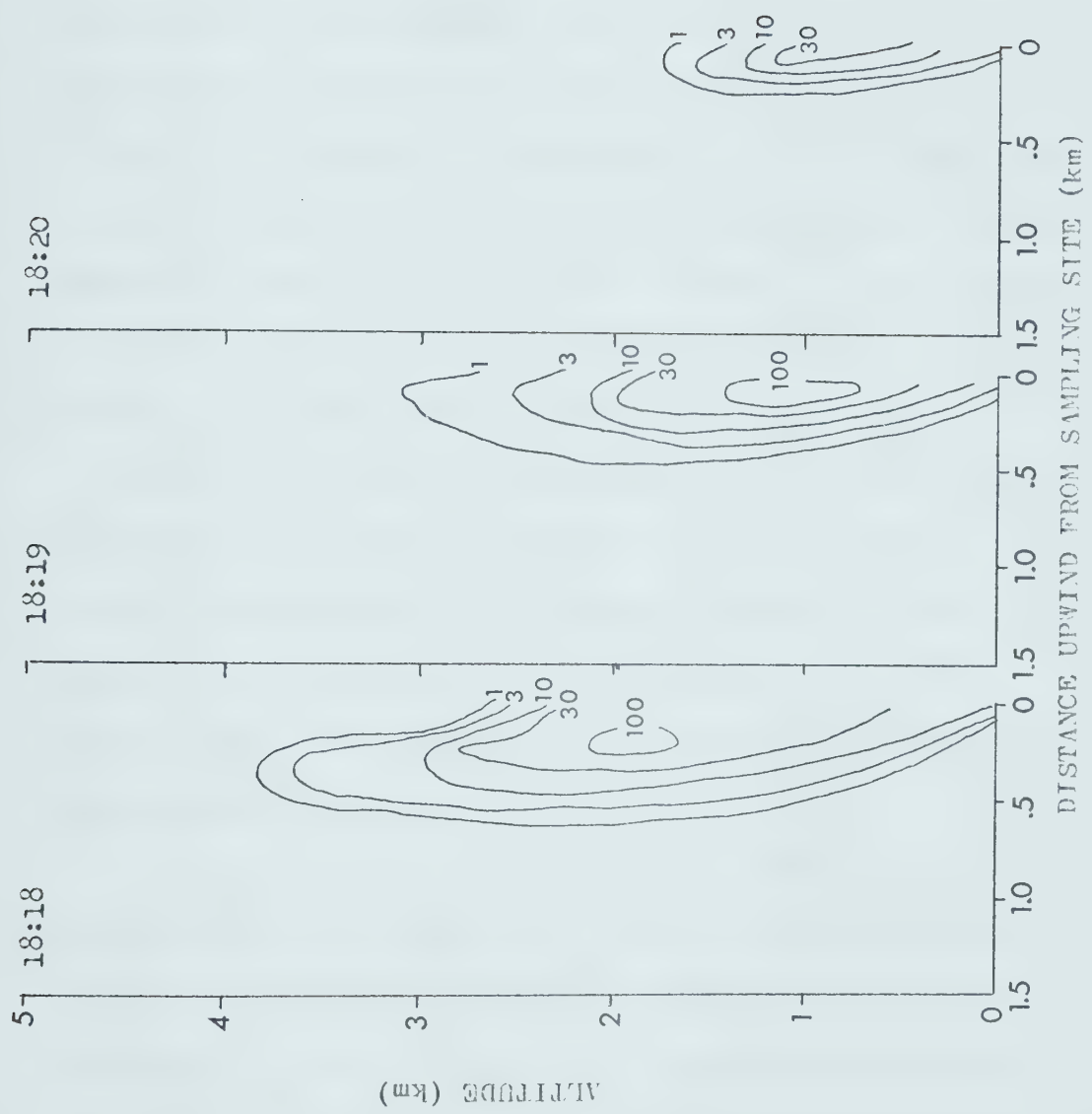














with respect to the ground. Because of the large terminal velocity and the small concentration, this isolated area seems to consist of large hailstones. As seen in Figure 14, large hail fell in the later stages of this hailfall. The existence of local areas of concentration maxima may be detected in another way. Examining the concentrations at the 3 km level, it may be seen that the concentration at the beginning time of 18:08 is  $1 \text{ m}^{-3}$ . This concentration increases to  $3 \text{ m}^{-3}$  at 18:12, then suddenly to  $30 \text{ m}^{-3}$  at 18:13. The concentration decreases to  $10 \text{ m}^{-3}$  at 18:14, then increases again to  $30 \text{ m}^{-3}$  at 18:15. This concentration is maintained until about 18:18, when the concentration begins diminishing to 0 at 18:20. These regions of local concentration maxima may be the result of the passage of more than one hail cell.

Another feature is the observation that hail which falls at a point comes from a region of greater horizontal extent in the upper levels. In this example, the collected hailstones extend over a distance of about 1 km horizontally at the 3 km level at 18:16. This point is relevant to comparing hail measured on the ground with radar measurements aloft.

The model is principally limited by not having a mechanism for the growth or melting of hail. Another improvement might be to use exponential distributions as the input, rather than the experimental results. This would give smoother concentration fields at the expense of greater deviations from the real situation.



## CHAPTER 7. SUMMARY AND RECOMMENDATIONS

### 7.1 Summary

The field operations of the sequential sampling experiment were largely successful. Sequential hail samples were collected in three hailstorms in 1973 and six in 1974, indicating an improvement in hailstorm sampling ability partially due to increased experience. The best results were obtained when one person was able to devote most of his time to the sample collection. Collection of rainwater was the biggest difficulty with the equipment, but for the most severe storms, this problem was reduced. The large mesh size of the catcher netting did not appear to be a major factor in the non-capture of hail. Recording data on tape caused trouble on a few occasions.

The analysis techniques were less successful. The manual method of counting and measuring photographs of hailstones gives useful results, but is tedious. The computerized line scanning system is not much faster when all the necessary photographic steps are included, and it suffers from large calibration errors. Attempts at analyzing the internal structures of the hailstones were handicapped by the small hailstone sizes,



and by an inadequate hailstone sectioning method. The bandsaw used for sectioning could be used only on hailstones larger than about 1 cm in diameter, and the coarse teeth produced a rough surface.

The size distribution studies indicated that the hail was essentially exponentially distributed with size, with the degree of fit decreasing for smaller sizes. The dividing point for the accurate description by an exponential distribution is at about a diameter of 0.5 cm, corresponding to the MANOBS definition of hail. The exponential distribution of the total hail sample was given by

$$N(D) = 28,239 e^{-2.0D} \quad (32)$$

where  $D$  is in cm. For samples from the individual storms, the coefficient of the exponent varied from  $1.08 \text{ cm}^{-1}$  to  $5.83 \text{ cm}^{-1}$ .

Log-normal distributions also approximate the observed size spectra of hail, but with deviations for both large and small diameters of hailstones. About 65 percent of the measured particles were less than 0.5 cm in diameter. The log-normal distributions were also approximated by straight lines, and the slopes of these lines showed variation from 2.28 to 7.34.

Power law distributions best fit the expected size distribution of

$$C(D) = k D^{-3} \quad (55)$$

when the sample considered was limited to hailstones with diameters greater than about 1.0 cm. When the smaller hailstones were included, the exponent tended to have a value around 1.5.



The time-dependent study did not permit generalizations to be made about falling hail, because of the small number of storm samples studied. However, interesting deductions can be made on the basis of this limited information. It was found that the greatest values of hailstone number flux, and mean hailstone diameter tended to occur in the middle of a hailfall at a point. Number fluxes and concentrations at the ground reached maximum values of about 1000 hailstones  $\text{m}^{-2} \text{min}^{-1}$  and 2600 hailstones  $\text{m}^{-3}$ . These numbers may show a variation of a factor of ten from one sample to the next, so the instantaneous values may be considerably higher than the values given for 1 minute averages. The size distribution of the hail is most nearly exponential during the times of greatest hailstone flux. The changes of the size distribution of the falling hail with time may be partly due to the sorting of the hail with respect to size by the vertical shear of the horizontal wind.

The modelling of the upper level concentration of the hail samples was limited by the simplicity of the model. It showed that for the particular case modelled, the collected hailstones may have come from more than one distinct storm region. It also showed that hail at a point on the ground may have arrived from a region of greater horizontal extent at upper levels.



## 7.2 Recommendations

The only major improvement needed for the field operation of the experiment is some method of separating hail from the rain. A lot of effort has been devoted to this problem by the author and by the personnel at ALHAP, but no satisfactory simple solution has been found. A centrifuge may work, but it seems unnecessarily complicated for such a simple problem. If the person concerned with operating the sampling system must devote a large part of his time to other matters, then an automatic sample container switcher would be a useful feature. If the sizes of the hail are the only interest, then the experiment could be considerably simplified by making the photographs of the hail in the field, by photographing a dark background that has been left out in the hailfall a known time. Schemenaur (1974) used a similar method for graupel. For internal analysis, the hailstones will have to be collected. Federer and Waldvogel (1975) give a brief description of a hailstone spectrometer used to collect sequential samples in Switzerland.

For the analysis of size distributions of collected hail, the greatest improvement would be to correctly calibrate the computer line scanning system. The problems of the system that were mentioned in Chapter 3 could be reduced by using sample sizes consisting of fewer hailstones. These smaller samples would be representative fractions of the collected samples. Alternatively, the collected sample could be divided into subsamples, each of which would be analyzed and then added to-



gether. A television camera could be used to photograph the hail samples and the resulting signal fed directly into the computer, thereby eliminating considerable noise and processing time.

In order to clarify the points raised in Chapter 5 about the time-dependent properties of falling hail, more sequential storm samples should be studied. The three cases studied were subjectively picked to cover a wide range of storm severities, but perhaps they were not representative of the full diversity of hailstorms. The variation with time of the correlation coefficients among various parameters should be studied in greater detail. In particular, it was suggested in Chapter 5 that hailstone number flux and mean diameter may correlate well only during the most intense hailfall. Although there is no reason for two parameters to be constantly correlated throughout a hailfall, there may exist correlations for part of the time.

The model of falling hail needs growth and melting processes included in its equations. In addition, a more detailed wind structure and temperature profile should be used, and may be available from mobile radiosonde soundings. The model uses the hailfall at one point only, so an estimate of the areal extent of the fallen hail could be used to calculate more realistic values of actual upper level concentrations. Alternatively, a set of sequential samples could be obtained from many points.



Analysis of other hailstone parameters, such as axis ratios, surface roughnesses, and internal structure, will depend largely on the availability of a suitable sample consisting of large, well-preserved hailstones. Measurements of the surface roughness and axis ratios would enable better estimates of drag coefficients as well as an evaluation of the factors used in the heat transfer equations used in the study of melting hailstones. The analysis of the internal structure of the hailstones may make it possible to determine the growth environment of the hailstones, but that will depend on the availability of suitable hailstones and analysis equipment.



## BIBLIOGRAPHY

1. Atlas, D., 1963: Severe Local Storms. Meteorological Monographs, Vol. 5, 247 pp.
2. Atlas, D., and F. Ludlam, 1961: Multi-wavelength Radar Reflectivity of Hailstones, Quarterly Journal of the Royal Meteorological Society, 87, 523-534.
3. Auer, A., 1972: Distribution of Graupel and Hail with Size. Monthly Weather Review, 100, 325-328.
4. Auer, A., and J. Marwitz, 1972: Hail Encountered in the Vicinity of Thunderstorm Updrafts. Journal of Applied Meteorology, 11, 748-752.
5. Barge, B., and G. Isaac, 1973: The Shape of Alberta Hailstones. Journal de Recherches Atmosphériques, 7, 11-20.
6. Battan, L., and J. B. Theiss, 1972: Observed Doppler Spectra of Hail. Journal of Applied Meteorology, 11, 1001-1007.
7. Chapman, D. G., and R. A. Schauffele, 1970: Elementary Probability Models and Statistical Inference, Xerox Publishing, 358 pp.
8. Charlton, R. B., and R. List, 1972: Hail Size Distributions and Accumulation Zones. Journal of the Atmospheric Sciences, 29, 1182-1193.
9. Dennis, A. S., 1971: Hailstone Size Distributions and Equivalent Radar Reflectivity Factors Computed from Hailstone Momentum Records. Journal of Applied Meteorology, 10, 79-85.
10. Douglas, R. H., 1960: Size Distributions, Ice Contents, and Radar Reflectivities of Hail in Alberta. Nubila, III, 5-11.
11. Douglas, R. H., 1963: Size Distributions of Alberta Hail Samples. Scientific Report MW-36, Stormy Weather Research Group, McGill University, Montreal, 55-70A.



12. Douglas, R. H., 1964: Hail Size Distributions. Proceedings of the 1964 World Conference on Radar Meteorology, Boulder, Colorado, 146-149.
13. Federer, B., and A. Waldvogel, 1975: Hail and Raindrop Size Distributions From a Swiss Multicell Storm. Journal of Applied Meteorology, 14, 91-97.
14. Iribarne, J. and R. de Pena, 1962: The Influence of Particle Concentration on the Evolution of Hailstorms. Nubila, V, 7-30.
15. Joss, J., and A. Waldvogel, 1969: Raindrop Size Distributions and Sampling Size Errors. Journal of the Atmospheric Sciences, 26, 566-569.
16. Knight, C. A., and N. C. Knight, 1968: The Final Freezing of Spongy Ice: Hailstone Collection Techniques and Interpretations of Structure. Journal of Applied Meteorology, 7, 875-881.
17. List, R., R. B. Charlton and P. Buttuls, 1968: A Numerical Experiment on the Growth and Feedback Mechanisms of Hailstones in a One-Dimensional Steady-State Model Cloud. Journal of the Atmospheric Sciences, 25, 1061-1074.
18. List, R., and J-G. Dussault, 1967: Quasi-Steady State Icing and Melting Conditions and Heat and Mass Transfer of Spherical and Spheroidal Hailstones. Journal of the Atmospheric Sciences, 24, 522-529.
19. List, R., W. A. Murray, and C. Dyck, 1972: Air Bubbles in Hailstones. Journal of the Atmospheric Sciences, 29, 916-920.
20. Lozowski, E. P., M. M. Oleskiw, and T. M. Morrow, 1975: Hail Photography: An Example of the Use of High-Speed Techniques Under Adverse Conditions. Journal of the Society of Motion Picture and Television Engineers, 84, 18-24.
21. Ludlam, F. and W. C. Macklin, 1960: Some Aspects of a Severe Storm in S. E. England. Nubila, II, 38-50.
22. MANOBS: Manual of Standard Procedures for Surface Weather Observing and Reporting, Atmospheric Environment Service, Toronto, 307 pp.



23. Marshall, J. S., and W. McK. Palmer, 1948: The Distribution of Raindrops with Size. Journal of Meteorology, 5, 165-166.
24. Mason, B. J., 1956: On the Melting of Hailstones. Quarterly Journal of the Royal Meteorological Society, 82, 209-216.
25. Pell, J., 1971: Variations with Time of Six Alberta Hail Parameters. Proceedings of the Seventh Conference on Severe Local Storms, American Meteorological Society, Kansas City, 63-70.
26. Schemenauer, R. S., 1974: Size Distributions and Number Concentrations of Graupel from Alberta Showers. Preprint Volume, Conference on Cloud Physics, Tucson, Arizona, October 21-24, 1974. Published by the American Meteorological Society, Boston, MA.
27. Strong, G. S., 1974: The Objective Measurement of Alberta Hailfall, unpublished M. Sc. thesis, University of Alberta, 182 pp.
28. Sulakvelidze, G. K., 1967: Formation of Precipitation and Modification of Hail Processes, Israel Program for Scientific Translation, 207 pp.
29. Tsang, N., 1974: Determination of Hailpad Impression Size by Digital Picture Processing. Unpublished report to the Department of Computing Science, University of Alberta, 46 pp.
30. Ulbrich, C. W., 1974: Analysis of Doppler Radar Spectra of Hail. Journal of Applied Meteorology, 13, 387-396.
31. Ulbrich, C. W., D. Atlas and R. E. Rinehart, 1975: Hail Parameter Diagram. NHRE Symposium/Workshop on Hail, Estes Park, Colorado, September 21-28, 1975, Preprint Vol. 1.
32. Williams, G. N. and Douglas, R. H., 1963: Continuity of Hail Production in Alberta Storms. Scientific Report MW-36, Stormy Weather Research Group, McGill University, Montreal, 16-54.
33. Wisner, C., H. Orville and C. Myers, 1972: A Numerical Model of a Hail Bearing Cloud. Journal of the Atmospheric Sciences, 29, 1160-1181.



## APPENDIX I

### SAMPLING PROBLEMS



Various problems affected the collection of the sequential samples, thereby affecting the analyses. The troubles were the following ones.

1. 23 August 1973. Rain was collected along with hail in several of the samples, causing some melting and refreezing of the collected hailstones. This would alter the sample distribution leaving smaller hailstones overall, and fewer small hailstones than was actually the case.
2. 27 August 1973. Very soft, wet hail was collected, which was quite fragile in storage. Consequently, there was a lot of hailstone chipping and frost in the analyzed samples. The effect on the distribution would be to produce an excess of small hailstones.
3. 24 June 1974. The sampling location was on the edge of the storm and no samples were obtained from the area of the most intense hailfall. Consequently, the collected samples may have represented hailstones smaller than average for that storm.
4. 2 July 1974. The timing of the samples was not recorded. However, since the total time of sampling was recorded as 1 minute for four samples, each was assumed to be 15 seconds long.
5. 9 July 1974. Sampling took place in the final stages of the hailstorm. The samples collected consisted mostly of rainwater which melted the hailstones to some extent, and spoiled any mass measurements. The resulting distribution would have been altered in a fashion similar to that for 23 August 1973.
6. 18 August 1974. The catcher net was torn by the large



hail. The rips were so large that particular size categories were probably not preferentially lost through the holes in the catcher net. The collection efficiency of the catcher was probably reduced to about one half. Sample spectra were probably not significantly affected, but the flux densities would have been reduced.



## APPENDIX II

### THE MELTING OF FALLING HAILSTONES



The problem of the melting of a hailstone as it falls below the freezing level has been considered by several authors (Mason, 1956; and List and Dussault, 1957). Mason (1956) gives the result that a particle with a radius of less than about 0.4 cm would melt completely on falling from a freezing level at 4 km above ground level in air with a lapse rate of  $6.5 \text{ C km}^{-1}$ .

A comprehensive treatment of the heat transfer between a hailstone and its environment is given by List and Dussault (1967). For a hailstone, there are four sources and sinks of heat, described by the following expressions.

1. Heat source from the freezing of accreted water.

$$Q_F = 0.785 \nu E W_f D R_e L_f I \quad (\text{A1})$$

2. Heat sink to warm the accreted cloud droplets.

$$Q_{CP} = -0.785 \nu E W_f D R_e \bar{c}_w (T_0 - T_A) \quad (\text{A2})$$

3. Heat sink by evaporation, condensation and sublimation.

$$Q_{ES} = -C_{1,2} \theta D_w a T_A^{-1} R_e^{\frac{1}{2}} D(e_{sn} - e_v) \delta X \quad (\text{A3})$$

4. Rate of heat transfer between a hailstone and its environment by conduction and convection.

$$Q_{CC} = -1.68 \theta k R_e^{\frac{1}{2}} D (T_0 - T_A) \delta X \quad (\text{A4})$$



where

$\nu$	is the kinematic viscosity of air
$E$	is the collection efficiency of the hailstone for cloud drops
$W_f$	is the free liquid water content of the air
$D$	is the major axis diameter of the hailstone (assumed oblate spherical)
$Re$	is the Reynolds number
$L_f$	is the latent heat of fusion at the deposit temperature
$I$	is the fraction of accreted water which freezes
$\overline{c_w}$	is the specific heat of water averaged over the temperature range $T_d$ to $T_a$
$T_D$	is the deposit steady state temperature
$T_A$	is the air temperature
$C_{i,2}$	is the latent heat of evaporation or sublimation
$\theta$	is the roughness factor
$D_{wa}$	is the diffusivity of water vapor in air
$e_{sh}$	is the saturation vapor pressure over the hailstone
$e_v$	is the partial pressure of water vapor in ambient air
$\gamma$	is the surface ratio of spheroid to a sphere
$\chi$	is the heat transfer factor for a spheroid
$k$	is the thermal conductivity of air.

When these equations are applied to melting, a few changes are required. The deposit temperature  $T_d$  remains constant at 0C. Because any water drops that are shed will be warmed by the air and not the hailstone, Equation A2 becomes



$$Q_{cp} = 0 \quad (A5)$$

Equation A1 becomes

$$Q_M = -0.785 \nu W_f' D R_e L_f \quad (A6)$$

where  $W_f'$  is the free liquid water produced in the wake of the hailstone by its melting. The collection efficiency in this case represents the divergence of the water droplets and water vapor in the wake of the hailstone and is approximately equal to 1.

For a steady state the sum of the heat sources and sinks is zero, or

$$Q_M + Q_{ES} + Q_{cc} = 0 \quad (A7)$$

This formulation neglects the heat required to raise the temperature of the interior of the hailstone to 0 C. When Equations A3, A4, A5 and A6 are substituted into Equation A7, the thermodynamic state of a hailstone below the freezing level can be described by (List and Dussault, 1967)

$$\frac{1.68k(T_0 - T_A) + C_{1,2} D_{wa} T_A^{-1} (e_{sh} - e_v)}{0.785 \nu L_f} = W_f' \Phi \quad (A8)$$

where

$$\Phi = \frac{E R_e^{\frac{1}{2}}}{\theta \gamma X} \quad (A9)$$



This leads to the following equation relating the diameter and the auxiliary function  $\Phi$  below the freezing level:

$$\Phi = 59.33 D^{\frac{3}{4}} \quad (\text{A10})$$

The liquid water content produced in the wake by the melting hailstone is given by

$$W_f' = \frac{1.68k(T_A - T_0) + C_{1,2} D_{wa} T_A^{-1} (e_{sh} - e_v)}{0.785 \times 59.33 \nu L_f D^{\frac{3}{4}}} \quad (\text{A11})$$

The terminal speed of a falling spherical hailstone can be found by Equation 18. The air temperature is given by

$$T_A = T_s - \Gamma Z \quad (\text{A12})$$

where  $\Gamma$  is the lapse rate, assumed constant at  $6.5 \text{ C km}^{-1}$ , and  $T_s$  is the surface air temperature. Using the above equations, the mass melted from a hailstone in a time interval  $\delta t$  is given by

$$\delta M = \frac{\pi D^2}{4} V_T \delta t W_f' \quad (\text{A13})$$

The change in diameter,  $\delta D$ , is given by

$$\delta D = \frac{2\delta M}{\pi D^2 \rho_i} \quad (\text{A14})$$



and the diameter after time  $\delta t$  is given by

$$D_{NEW} = D_{OLD} - \delta D \quad (A15)$$

This incremental procedure for the determination of the diameter of a melting hailstone as a function of time can be repeated until the hailstone either reaches the ground or melts completely.

Equations A11 to A16 were solved by computer with the following parameters. The air density was kept constant at a value of  $\rho_A = 1.05 \times 10^{-3} \text{ g cm}^{-3}$ . The effects of relative humidity or already present liquid water were ignored, which would increase the rate of melting. The hailstones were assumed to be smooth spheres with a drag coefficient of 0.5 and a density of  $0.89 \text{ g cm}^{-3}$ .

Table A1 shows the radius of the frozen part of a melting hailstone falling from the freezing level, upon reaching the ground.

---

		Initial radius (cm)			
		0.1	0.2	0.3	0.4
Freezing level (km)	1.0	0	0.13	0.26	0.36
	2.0	0	0	0	0.22
	3.0	0	0	0	0
	4.0	0	0	0	0

---

TABLE A1      Radius of the frozen part of a melting hailstone at the ground level after falling from the freezing level



Table A1 shows that for a radius less than about 0.4 cm a hailstone will melt completely while falling 3 km below the freezing level. The effects of melting become less significant as the diameter increases because the increased terminal velocity results in less time being spent in the air, and the greater mass requires more latent heat to melt the ice.

The liquid water content of the air produced by the melting hail is an interesting by-product of the solution of the equations. The values of  $W_f'$  are summarized in Table A2.

---

Initial radius (cm)	2.5	2.0	1.5	1.0	0.9	0.8	0.7	0.6	0.5
$W_f'$ ( $\text{g m}^{-3}$ )	2.5	3.0	3.5	5.1	5.7	6.5	7.4	9.7	18.5

---

TABLE A2    Liquid water concentrations produced at the ground in the wakes of melting hailstones.

Table A2 applies only in the wake of the falling hailstones, and so will not directly give the total water content of the air. However, it does show that showers of small hail may produce high liquid water contents, and, hence, high rainfall rates.

The effect of melting on a cumulative exponential distribution is shown in Figure A1. The hail size distribution at the freezing level is assumed to be exponential. The change in the smaller diameters (less than 0.5 cm) is qualitatively in agreement with that observed in the individual collected hail samples.



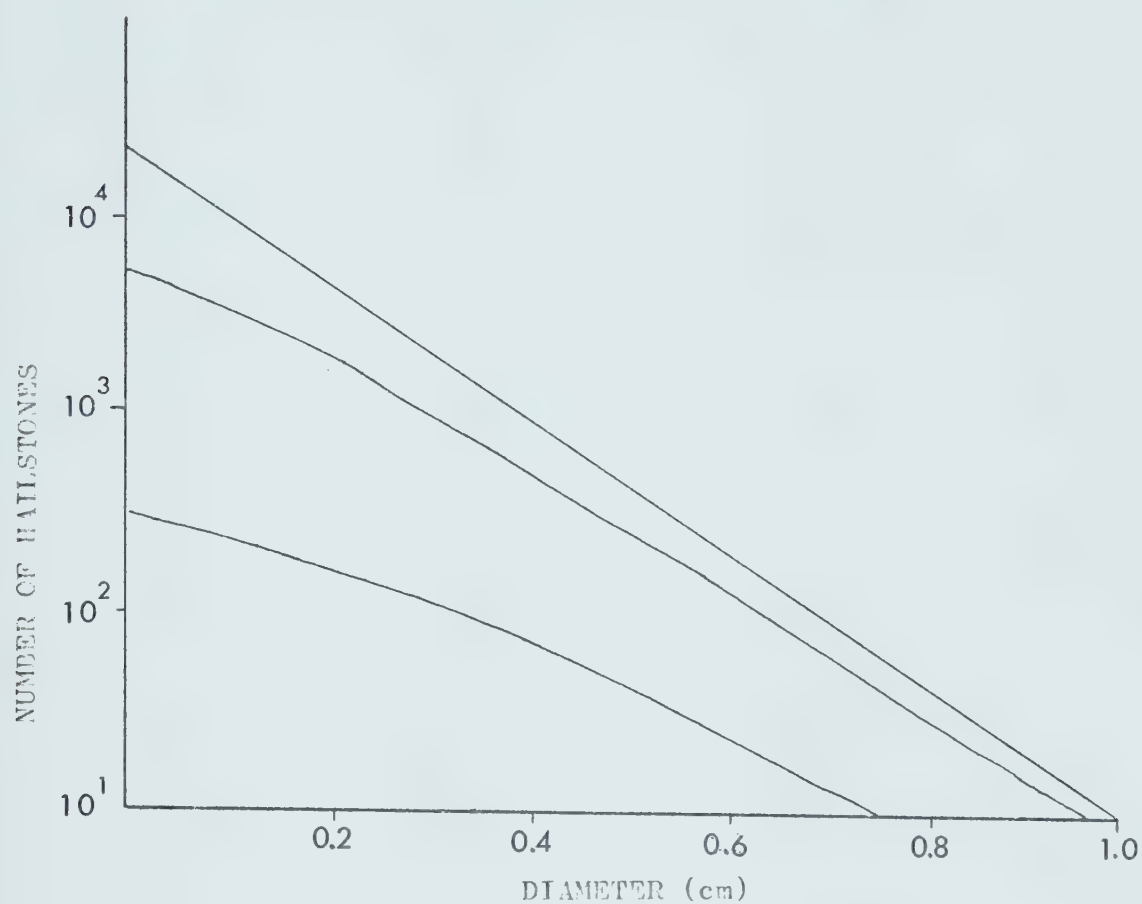


FIGURE A1. The effect of melting on a cumulative exponential distribution. The top curve is an initial distribution at the freezing level, assumed exponential. The middle curve is the resulting distribution if the freezing level is at 1.0 km, and the lower curve is the result if the freezing level is at 2.0 km.



APPENDIX III  
INDIVIDUAL SAMPLES --  
COLLECTION LOCATIONS AND TIMES,  
SAMPLE DESCRIPTIONS AND  
DISTRIBUTION PARAMETERS



LINE	SAMPLING DATE	SAMPLING LOCATION	SAMPLE CONTAINER	TIME OF SAMPLE START	TIME OF SAMPLE END	SAMPLE DURATION	SAMPLE MASS (G.)	NUMBER OF HAILSTONES	MEAN DIAMETER (CM)
1	23 JUL73	NW S27T38R08	BOTTLE	19:41:00	19:43:00	2:00	65.6	-0	-0.00
2				19:43:00	19:45:00	2:00	118.1	555	.30
3				19:45:00	19:47:00	2:00	18.5	415	.40
4	23 AUG73	SE S33T35R04	BOTTLE	17:50:00	17:50:15	0:15	112.8	1049	.30
5				17:50:15	17:50:30	0:15	133.1	1104	.30
6				17:50:30	17:50:45	0:15	152.5	1104	.30
7				17:50:45	17:51:15	0:30	37.4	-0	-0.00
8				17:51:15	17:51:45	0:30	30.4	21	.93
9				17:51:45	17:52:15	0:30	23.0	-0	-0.00
10				17:52:15	17:52:45	0:30	14.0	36	.77
11				17:52:45	17:54:00	1:15	-0.0	-0	-0.00
12	27 AUG73	SE S33T35R04	BOTTLE	15:23:00	15:23:20	0:20	32.1	231	.31
13				15:23:20	15:23:40	0:20	112.6	-0	-0.00
14				15:23:40	15:24:00	0:20	16.5	-0	-0.00
15				15:24:00	15:24:20	0:20	26.1	-0	-0.00
16				15:24:20	15:24:40	0:20	13.5	-0	-0.00
17				15:24:40	15:25:00	0:20	51.9	157	.41
18				15:25:00	15:25:20	0:20	63.2	185	.30
19				15:25:20	15:25:40	0:20	118.2	342	.81
20				15:25:40	15:26:00	0:20	159.7	392	.33
21				15:26:00	15:26:20	0:20	134.4	200	.39
22				15:26:20	15:26:40	0:20	63.7	259	.37
23				15:26:40	15:27:00	0:20	46.8	176	.56
24				15:27:00	15:27:20	0:20	98.0	385	.45



LINE	SAMPLING DATE	SAMPLING LOCATION	SAMPLE CONTAINER	TIME OF SAMPLE START	TIME OF SAMPLE END	SAMPLE DURATION	SAMPLE MASS (G.)	NUMBER OF HAILSTONES	MEAN DIAMETER (CM)
25				15:27:20	15:27:40	0:20	147.5	408	.40
26				15:27:40	15:28:00	0:20	77.0	297	.50
27				15:28:00	15:28:20	0:20	97.5	212	.41
28				15:28:20	15:28:40	0:20	92.7	241	.44
29				15:28:40	15:29:00	0:20	118.2	443	.45
30				15:29:00	15:29:20	0:20	132.1	766	.40
31				15:29:20	15:29:40	0:20	103.1	897	.33
32				15:29:40	15:30:00	0:20	83.1	411	.53
33				15:30:00	15:30:20	0:20	20.7	17	.71
34	24 JUN74	NE S09T31R03	BOTTLE	15:55:30	15:56:00	0:30	11.4	55	.79
35				15:56:00	15:56:30	0:30	10.6	50	.79
36				15:56:30	15:57:00	0:30	5.1	25	.83
37				15:57:00	15:58:00	1:00	1.0	9	.62
38				15:58:00	15:59:00	1:00	0.0	3	.57
39				15:59:00	16:00:00	1:00	0.0	5	.50
40	02 JUL74	SF S26T38P03	BOTTLE	17:25:00	17:25:15	0:15	98.5	44	.16
41				17:25:15	17:25:30	0:15	1.0	11	.48
42				17:25:30	17:25:45	0:15	1.8	3	.90
43				17:25:45	17:26:00	0:15	4.0	74	.12
44	05 JUL74	NW S36T38R02	BOTTLE	16:47:00	16:48:30	1:30	1.5	49	.56
45				16:48:30	16:50:30	2:00	10.2	259	.45
46				16:50:30	16:51:40	1:10	.1	51	.24
47				16:51:40	16:53:40	2:00	10.1	159	.48
48				16:54:05	16:56:00	1:55	3.2	198	.35
49				16:56:00	16:57:00	1:00	.1	1	1.10



LINE	SAMPLING DATE	SAMPLING LOCATION	SAMPLE CONTAINER	TIME OF SAMPLE START	TIME OF SAMPLE END	SAMPLE DURATION	SAMPLE MASS (G.)	NUMBER OF HAILSTONES	MEAN DIAMETER (CM)
50	09 JUL 74	NW S36T38R02	HEAKER	22:03:00	22:05:00	2:00	-0.0	-0	-0.00
51				22:05:00	22:07:00	2:00	-0.0	34	.34
52				22:07:00	22:09:00	2:00	-0.0	72	.43
53				22:09:00	22:10:30	1:30	-0.0	14	.47
54				22:10:30	22:13:00	2:30	-0.0	81	.28
55				22:13:00	22:16:00	3:00	-0.0	39	.30
56	18 AUG 74	SW S24T34R01	HAG	17:21:00	17:24:15	3:15	355.0	122	2.05
57				17:24:15	17:26:15	2:00	360.8	50	2.28
58				17:26:15	17:27:15	1:00	242.9	36	3.12
59				17:27:15	17:28:15	1:00	128.2	24	2.75
60				17:28:15	17:29:15	1:00	53.3	41	1.49
61				17:29:25	17:30:15	1:00	12.4	25	1.02
62				17:30:15	17:33:45	3:30	-0.0	14	.80
63	18 AUG 74	S36T33R28	HAG	17:49:00	17:51:00	2:00	4.5	20	.85
64				17:51:00	17:54:00	3:00	-0.0	-0	-0.00
65	18 AUG 74	SW S23T33R26	HAG	18:10:00	18:15:00	5:00	10.0	73	.70
66				18:15:00	18:16:00	1:00	49.6	70	1.16
67				18:16:00	18:17:00	1:00	387.5	497	1.18
68				18:17:00	18:18:00	1:00	341.4	283	1.33
69				18:18:00	18:19:00	1:00	652.7	739	1.22
70				18:19:00	18:20:00	1:00	197.1	395	.99
71				18:20:00	18:25:00	5:00	42.0	31	1.46
72				18:25:00	18:27:30	2:30	12.0	19	1.20
73	18 AUG 74	S01T33R25	HAG	18:42:30	18:44:30	2:00	-0.0	18	1.13
74				18:49:30	18:50:30	1:00	-0.0	-0	-0.00







FLUX DENSITY  
EXPONENTIAL DISTRIBUTION

CONCENTRATION  
EXPONENTIAL DISTRIBUTION

LINE	CUMULATIVE EXPONENTIAL				EXPONENTIAL				CUMULATIVE EXPONENTIAL				EXPONENTIAL			
	N	LAMBDA (CM-1)	S	2	N	LAMBDA (CM-1)	S	2	N	LAMBDA (CM-1)	S	2	N	LAMBDA (CM-1)	S	2
25	2074	3.654	.30	4.05	3456	3.668	.30	3.113	429	3.113	4.05	3456	722	3.143	.30	4.27
26	1396	2.540	1.16	6.32	2348	2.579	1.31	1.948	187	1.948	6.32	2348	314	1.971	1.31	6.76
27	2489	3.307	1.72	5.11	4142	3.307	1.72	2.641	417	2.641	5.11	4142	695	2.641	1.72	5.10
28	1500	3.924	2.76	4.16	2694	3.972	3.03	2.786	239	2.786	4.16	2694	402	2.821	3.03	4.36
29	2415	3.364	1.02	5.27	4078	3.445	1.11	2.770	423	2.770	5.27	4078	719	2.821	1.11	5.52
30	3194	3.143	1.43	18.83	5313	3.148	1.44	2.887	570	2.887	18.83	5313	951	2.906	1.44	19.53
31	3311	3.408	1.65	25.50	5504	3.410	1.67	3.171	502	3.171	25.50	5504	989	3.196	1.67	26.66
32	2693	2.986	1.59	1.88	4566	3.016	1.79	2.335	441	2.335	1.88	4566	749	2.372	1.79	2.07
33	406	4.419	4.09	13.98	687	4.506	4.51	-3.91	5	-3.91	13.98	687	8	-4.31	4.51	15.74
34	394	2.257	1.31	3.44	648	2.254	1.32	-2.47	9	-2.47	3.44	648	15	-2.452	1.32	3.49
35	634	3.442	6.52	10.55	1049	3.454	6.42	.230	14	.230	10.55	1049	24	.251	6.42	10.52
36	456	3.758	3.24	16.27	753	3.751	3.23	.115	5	.115	16.27	753	9	.113	3.23	16.16
37	163	4.667	1.81	7.55	252	4.582	1.70	.150	5	.150	7.55	252	9	.117	1.70	6.87
38	14	2.130	.80	0.00	24	2.130	.80	0.000	2	0.000	0.00	24	4	0.000	.80	0.00
39	99	5.816	.03	.97	149	5.648	.02	3.026	19	3.026	.97	149	28	2.816	.02	.84
40	415	11.680	9.99	20.43	692	15.851	11.98	11.775	209	11.775	20.43	692	350	11.925	11.98	20.88
41	113	3.212	3.37	7.62	187	3.210	3.33	.431	10	.431	7.62	187	16	.426	3.33	7.49
42	-0	-0.000	-0.00	-0.00	-0	-0.000	-0.00	-0.000	-0	-0.000	-0.00	-0	-0	-0.000	-0.00	-0.00
43	-0	-0.000	-0.00	-0.00	-0	-0.000	-0.00	-0.000	-0	-0.000	-0.00	-0	-0	-0.000	-0.00	-0.00
44	127	4.133	4.64	12.36	210	4.198	5.08	.018	5	.018	12.36	210	7	-.044	5.08	13.38
45	362	5.086	5.07	23.54	607	5.165	5.38	1.257	21	1.257	23.54	607	35	1.326	5.38	24.10
46	84	6.261	.59	5.48	138	6.383	.67	3.933	26	3.933	5.48	138	43	4.119	.67	6.15
47	319	4.757	2.31	4.82	529	4.812	2.42	2.213	36	2.213	4.82	529	60	2.275	2.42	5.32
48	334	6.852	3.95	23.25	563	7.014	4.25	3.493	39	3.493	23.25	563	66	3.661	4.25	24.09
49	-0	-0.000	-0.00	-0.00	-0	-0.000	-0.00	-0.000	-0	-0.000	-0.00	-0	-0	-0.000	-0.00	-0.00







## LOG-NORMAL DISTRIBUTION PARAMETERS

LINE	SLOPE	PROBABILITY D < 0.1 cm	VARIANCE	MEDIAN DIAMETER (CM)
1	-0.00	-0.00	-0.0	-0.000
2	3.32	.09	9.4	.250
3	4.34	.02	13.3	.299
4	3.54	.09	10.2	.243
5	3.06	.13	17.3	.234
6	3.10	.14	14.3	.228
7	-0.00	-0.00	-0.0	-0.000
8	6.24	0.00	38.6	.753
9	-0.00	-0.00	-0.0	-0.000
10	13.88	0.00	27.7	.688
11	-0.00	-0.00	-0.0	-0.000
12	3.47	.14	17.9	.202
13	-0.00	-0.00	-0.0	-0.000
14	-0.00	-0.00	-0.0	-0.000
15	-0.00	-0.00	-0.0	-0.000
16	-0.00	-0.00	-0.0	-0.000
17	3.96	.04	13.1	.282
18	4.15	.11	13.8	.199
19	3.68	0.00	14.6	.550
20	3.43	.13	13.0	.214
21	3.51	.17	11.6	.262
22	3.90	.06	19.9	.249
23	3.52	.02	11.4	.402
24	3.32	.06	17.1	.290



## LOG-NORMAL DISTRIBUTION PARAMETERS

LINE	SLOPE	PROBABILITY D < 0.1 cm	VARIANCE	MEDIAN DIAMETER (CM)
25	3.38	.08	7.5	.263
26	3.18	.05	12.5	.331
27	3.13	.10	20.5	.258
28	3.70	.04	23.0	.289
29	3.60	.04	7.9	.310
30	3.07	.11	10.3	.254
31	2.77	.22	12.1	.191
32	3.43	.04	21.7	.337
33	11.50	0.00	36.3	.620
34	6.61	0.00	45.7	.655
35	7.18	0.00	28.1	.657
36	9.27	0.00	22.8	.731
37	12.93	0.00	20.9	.537
38	7.85	0.00	200.3	.379
39	15.07	0.00	6.8	.426
40	7.17	.40	10.6	.108
41	5.20	0.00	80.0	.353
42	-0.00	-0.00	-0.0	-0.000
43	-0.00	-0.00	-0.0	-0.000
44	5.02	0.00	22.1	.410
45	5.39	.17	15.8	.336
46	4.86	0.00	52.0	.158
47	5.52	.02	8.8	.384
48	4.77	.03	6.0	.265
49	-0.00	-0.00	-0.0	-0.000



## LOG-NORMAL DISTRIBUTION PARAMETERS

LINE	SLOPE	PROBABILITY D < 0.1 cm	VARIANCE	MEDIAN DIAMETER (CM)
50	-0.00	-0.00	-0.0	-0.000
51	4.93	.01	27.2	.236
52	4.69	0.00	15.6	.312
53	5.30	.04	45.4	.348
54	5.56	.01	25.7	.207
55	7.37	0.00	34.4	.217
56	5.16	0.00	14.5	1.774
57	5.77	0.00	34.5	1.932
58	13.82	0.00	13.7	2.932
59	7.85	0.00	20.8	2.484
60	6.64	0.00	32.6	1.283
61	13.06	0.00	6.5	.931
62	8.62	0.00	21.5	.649
63	10.03	0.00	16.4	.730
64	-0.00	-0.00	-0.0	-0.000
65	9.54	0.00	42.8	.599
66	9.52	0.00	20.6	1.052
67	8.03	0.00	10.4	1.049
68	7.96	0.00	7.6	1.210
69	6.71	0.00	8.3	1.101
70	7.08	0.00	15.0	.870
71	14.95	0.00	48.4	1.353
72	17.42	0.00	70.1	1.085
73	12.02	0.00	11.1	1.035
74	-0.00	-0.00	-0.0	-0.000



## APPENDIX IV

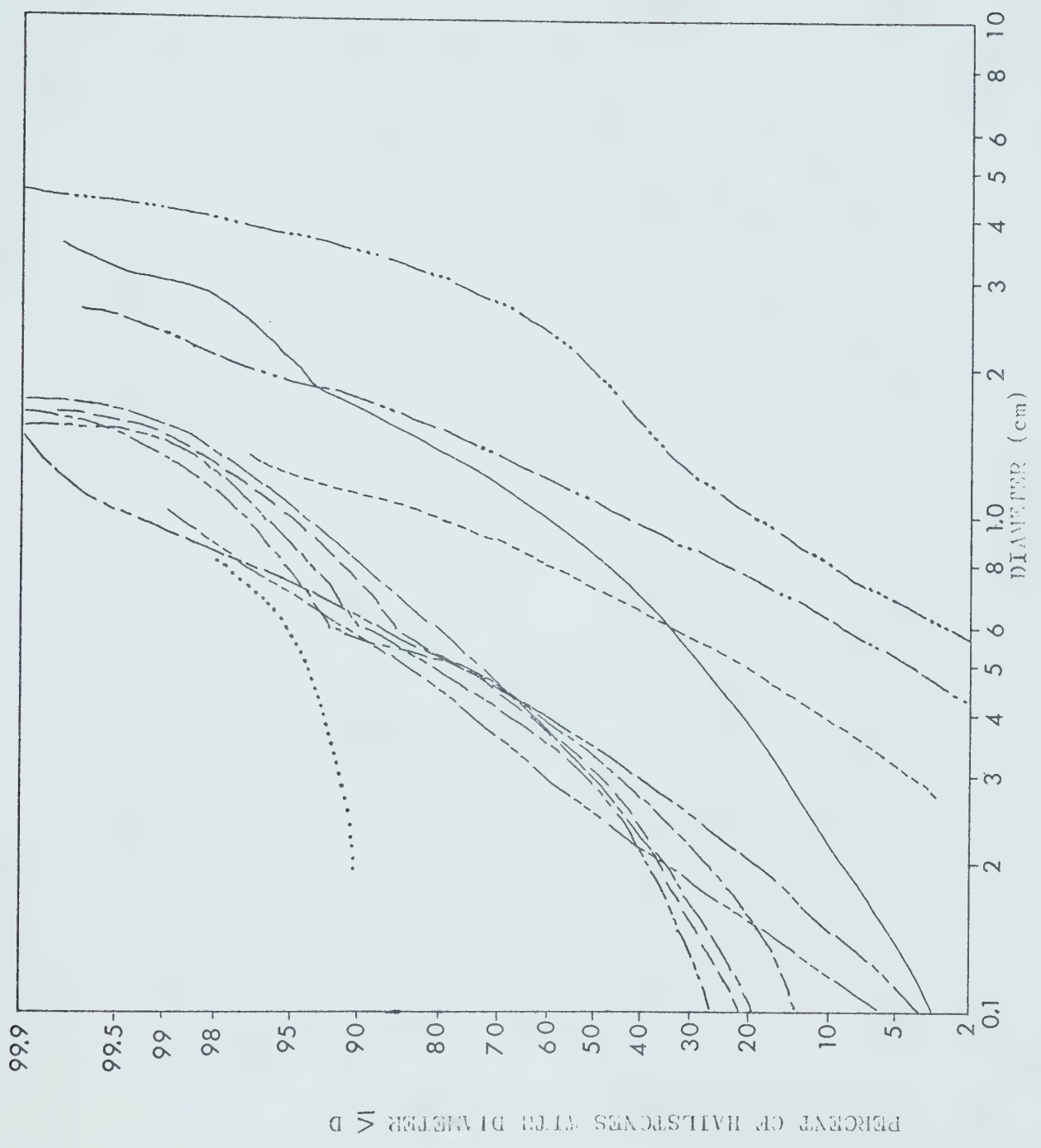
### LOG-NORMAL DISTRIBUTIONS FOR INDIVIDUAL STORM SAMPLES



FIGURE A2. Log-normal size distributions of the hail collected at individual sample sites. The lines correspond to the following sampling occasions.

\_\_\_\_\_ 1973  
 \_\_\_\_\_ 1974  
 \_\_\_\_\_ 23 July 1973  
 \_\_\_\_\_ 23 August 1973  
 \_\_\_\_\_ 27 August 1973  
 ..... 2 July 1974  
 ----- 24 June 1974  
 ----- 5 July 1974  
 ----- 9 July 1974  
 ..... 18 August 1974  
 .. --- .. 18 August 1974







APPENDIX V  
FLUX DENSITY,  
CONCENTRATION  
AND SIZE SPECTRA  
OF SEQUENTIAL HAIL SAMPLES















## HAILSTONE DIAMETER (MM)

LINE	1	2	3	4	5	6	7	8	9	10	11	12	13	14	15
25	252	311	274	222	278	96	40	36	40	36	12	16	8	4	12
26	137	157	311	133	72	60	68	92	36	28	4	20	24	0	12
27	514	275	206	266	91	155	45	119	16	64	27	16	45	9	9
28	145	185	129	64	145	121	52	15	40	32	12	12	8	4	0
29	157	290	220	428	145	133	113	72	52	32	52	12	8	0	4
30	723	422	101	723	404	351	32	76	36	20	4	36	8	56	8
31	1551	652	317	141	161	727	15	44	24	4	32	56	4	24	24
32	242	272	0	242	214	202	113	101	76	0	60	28	28	24	20
33	0	0	0	4	4	12	25	4	12	4	0	0	0	0	0
34	0	0	0	20	10	20	31	13	24	20	20	20	0	0	0
35	0	0	5	6	20	17	27	24	13	27	13	10	3	0	0
36	0	0	0	3	3	3	24	10	24	3	6	3	3	0	0
37	0	0	0	3	7	7	10	0	3	0	0	0	0	0	0
38	0	0	3	0	0	3	0	3	0	0	0	0	0	0	0
39	0	0	0	7	7	0	3	0	0	0	0	0	0	0	0
40	137	151	13	0	0	0	0	0	0	0	0	0	0	0	0
41	0	26	6	6	6	6	20	6	0	0	0	0	0	0	0
42	0	0	0	0	0	0	0	0	20	0	0	0	0	0	0
43	347	117	0	0	0	0	0	0	0	0	0	0	0	0	0
44	1	2	4	10	11	11	3	8	2	0	0	0	0	1	0
45	3	16	34	36	37	25	13	6	1	2	0	0	0	0	0
46	20	25	17	4	7	0	0	0	0	0	0	0	0	0	0
47	1	19	19	19	31	18	14	4	5	0	0	0	0	0	0
48	6	42	53	34	24	7	2	2	0	1	0	0	0	0	0























## HAILSTONE DIAMETER (MM)

LINE	1	2	3	4	5	6	7	8	9	10	11	12	13	14	15
1	0	0	0	0	0	0	0	0	0	0	0	0	0	0	0
2	118	78	45	136	45	45	8	10	5	1	3	6	1	5	3
3	30	57	100	98	61	30	3	8	5	1	3	6	0	0	0
4	1856	1055	1120	1910	1150	523	50	195	80	60	43	61	8	28	43
5	2151	255	1053	1341	1003	1535	61	141	60	60	88	88	88	61	106
6	2709	1218	523	2401	1030	515	123	230	68	70	8	61	61	123	106
7	0	0	0	0	0	0	0	0	0	0	0	0	0	0	0
8	0	0	0	13	0	13	5	8	3	13	0	13	0	8	0
9	0	0	0	0	0	0	0	0	0	0	0	0	0	0	0
10	0	0	0	0	0	43	53	21	13	0	26	6	0	0	0
11	0	0	0	0	0	0	0	0	0	0	0	0	0	0	0
12	630	370	248	150	100	100	46	20	13	20	13	6	0	0	0
13	0	0	0	0	0	0	0	0	0	0	0	0	0	0	0
14	0	0	0	0	0	0	0	0	0	0	0	0	0	0	0
15	0	0	0	0	0	0	0	0	0	0	0	0	0	0	0
16	0	0	0	0	0	0	0	0	0	0	0	0	0	0	0
17	100	215	155	221	80	120	113	6	13	13	13	6	0	0	0
18	302	146	360	261	26	35	13	0	0	6	0	0	0	0	0
19	0	255	315	0	291	221	0	255	0	248	221	0	153	0	85
20	726	251	545	248	301	30	145	40	53	0	20	13	6	6	0
21	241	376	565	261	146	158	60	100	20	33	33	6	0	0	0
22	255	456	221	205	201	120	53	33	53	53	6	6	0	0	0
23	0	153	456	0	188	53	0	53	0	53	53	0	40	0	20
24	525	423	301	248	248	155	175	160	60	53	80	40	13	20	0











## HAILSTONE DIAMETER (MM)

LINE	1	2	3	4	5	6	7	8	9	10	11	12	13	14	15
25	430	517	456	370	463	100	66	60	66	60	20	26	13	6	20
26	227	261	518	221	120	100	113	153	60	46	6	33	40	0	20
27	856	452	443	443	151	275	75	198	30	106	45	30	75	15	15
28	248	308	215	106	241	201	86	26	66	53	20	20	13	6	0
29	328	483	353	713	241	221	188	120	86	53	46	20	13	0	6
30	1265	713	258	1205	673	585	53	126	60	33	6	60	13	93	13
31	2268	1128	531	235	268	1211	26	73	40	6	53	93	6	40	40
32	403	463	0	403	356	330	188	168	126	0	100	46	46	40	33
33	0	0	0	6	6	20	46	6	20	6	0	0	0	0	0
34	0	0	10	33	16	33	51	21	40	33	33	33	0	0	0
35	0	0	10	10	33	28	45	40	21	45	21	16	5	0	0
36	0	0	0	5	5	5	40	16	40	5	10	5	5	0	0
37	0	0	0	5	11	11	16	0	5	0	0	0	0	0	0
38	0	0	5	0	0	5	0	5	0	0	0	0	0	0	0
39	0	0	0	11	11	0	5	0	0	0	0	0	0	0	0
40	227	251	21	0	0	0	0	0	0	0	0	0	0	0	0
41	0	35	10	10	10	10	33	10	0	0	0	0	0	0	0
42	0	0	0	0	0	0	0	0	33	0	0	0	0	0	0
43	655	175	0	0	0	0	0	0	0	0	0	0	0	0	0
44	1	3	6	16	18	18	5	13	3	0	0	0	0	1	0
45	5	26	36	60	61	43	21	10	1	3	0	0	0	0	0
46	34	41	20	6	11	0	0	0	0	0	0	0	0	0	0
47	1	31	31	31	51	30	23	6	8	0	0	0	0	0	0
48	10	70	78	56	40	11	3	3	0	1	0	0	0	0	0























## HAILSTONE DIAMETER (MM)

LINE	1	2	3	4	5	6	7	8	9	10	11	12	13	14	15
1	0	0	0	0	0	0	0	0	0	0	0	0	0	0	0
2	107	71	75	124	41	68	6	10	5	2	4	7	2	5	3
3	27	51	71	89	56	72	4	8	5	2	3	6	0	1	0
4	210	156	125	215	134	104	5	22	9	9	5	7	1	3	5
5	358	94	122	151	113	173	7	16	9	9	10	10	10	7	12
6	314	137	104	277	116	55	14	26	10	8	1	7	7	14	8
7	0	0	0	0	0	0	0	0	0	0	0	0	0	0	0
8	0	0	0	3	0	3	2	2	1	3	0	3	0	2	0
9	0	0	0	0	0	0	0	0	0	0	0	0	0	0	0
10	0	0	0	0	0	10	12	5	3	0	6	0	0	0	0
11	0	0	0	0	0	0	0	0	0	0	0	0	0	0	0
12	64	56	37	24	15	15	7	3	2	4	2	1	0	0	0
13	0	0	0	0	0	0	0	0	0	0	0	0	0	0	0
14	0	0	0	0	0	0	0	0	0	0	0	0	0	0	0
15	0	0	0	0	0	0	0	0	0	0	0	0	0	0	0
16	0	0	0	0	0	0	0	0	0	0	0	0	0	0	0
17	15	32	22	33	12	15	17	1	2	2	2	1	0	0	0
18	40	25	55	39	7	13	2	0	0	1	0	0	0	0	0
19	0	44	47	0	42	33	0	38	0	37	33	0	23	0	13
20	117	42	56	37	45	12	22	6	2	0	3	2	1	1	0
21	42	56	59	39	22	25	9	15	3	5	5	1	2	0	0
22	55	75	53	44	30	15	5	5	2	5	1	1	0	0	0
23	0	23	55	0	25	14	0	14	0	8	8	0	6	0	3
24	78	13	45	37	40	28	25	24	9	8	12	6	2	3	1











## HAILSTONE DIAMETER (MM)

LINE	1	2	3	4	5	6	7	8	9	10	11	12	13	14	15
25	64	77	58	55	64	24	10	9	10	9	3	4	2	1	3
26	34	39	77	33	18	15	17	23	9	7	1	5	6	0	3
27	56	50	29	29	10	18	5	13	2	7	3	2	5	1	1
28	37	46	32	16	36	30	13	4	10	2	3	3	2	1	0
29	49	72	57	106	36	33	28	18	13	8	13	3	2	0	1
30	179	106	40	179	100	47	8	19	9	8	13	9	2	1	2
31	337	189	79	35	40	160	4	11	6	1	1	14	1	6	6
32	60	69	0	60	53	50	29	25	19	0	15	7	7	6	5
33	0	0	0	1	1	3	7	1	3	1	0	0	0	0	0
34	0	0	2	6	3	0	9	2	7	6	6	6	0	0	0
35	0	0	2	2	6	5	8	7	4	2	2	3	1	0	0
36	0	0	0	1	1	1	7	3	7	1	2	1	1	0	0
37	0	0	0	1	2	2	3	0	1	0	0	0	0	0	0
38	0	0	1	0	0	1	0	1	0	0	0	0	0	0	0
39	0	0	0	2	2	0	1	0	0	0	0	0	0	0	0
40	20	22	2	0	0	0	0	0	0	0	0	0	0	0	0
41	0	5	1	1	1	1	3	1	0	0	0	0	0	0	0
42	0	0	0	0	0	0	0	0	3	0	0	0	0	0	0
43	57	17	0	0	0	19	3	7	0	0	0	0	0	1	0
44	1	2	4	9	10	38	20	9	2	0	0	0	0	0	0
45	5	24	50	53	55	38	20	9	2	3	0	0	0	0	0
46	14	17	12	3	5	0	0	0	0	0	0	0	0	0	0
47	2	23	23	23	36	21	17	5	6	1	1	1	0	0	0
48	7	48	50	39	27	3	3	3	1	2	0	0	0	0	0

































**B30144**